ALK-positive histiocytosis: a new clinicopathologic spectrum highlighting neurologic involvement and responses to ALK inhibition

Kemps, P.G.; Picarsic, J.; Durham, B.H.; Helias-Rodzewicz, Z.; Hiemcke-Jiwa, L.; Bos, C. van den; ... ; Emile, J.F.

blood®
Regular Article

MYELOID NEOPLASIA

ALK-positive histiocytosis: a new clinicopathologic spectrum highlighting neurologic involvement and responses to ALK inhibition

Paul G. Kemps,[1,2,*] Jennifer Picarsic,[3,*] Benjamin H. Durham,[4,5] Zofia Hélias-Rodzewicz,[6,7] Laura Hiemcke-Jiwa,[2] Cor van den Bos,[2,8] Marianne D. van de Wetering,[2,8] Carel J. M. van Noesel,[9] Jan A. M. van Laar,[10,11] Robert M. Verdijk,[12] Uta E. Flucke,[13] Pancras C. W. Hogendoorn,[1] F. J. Sherida H. Woei-A-Jin,[14] Raf Sciot,[15] Andreas Beilken,[16] Friedrich Feuerhake,[17] Martin Ebinger,[18] Robert Möhle,[19] Falko Fend,[20] Antje Bornemann,[20] Verena Wiegering,[21] Karen Ernestus,[22] Tina Méry,[23] Olga Gryniewicz-Kwiatkowska,[24] Bozenna Dembowska-Baginska,[24] Dmitry A. Evseev,[25] Vsevolod Potapenko,[26,27] Vadim V. Baykov,[28] Stefania Gaspari,[29] Sabrina Rossi,[30] Marco Gessi,[31] Gianpiero Tamburrini,[32] Sébastien Héritier,[33] Jean Donadieu,[7,33] Jacinthe Bonneau-Lagacherie,[34] Claire Lamaison,[35] Laure Farnault,[36] Sylvie Fraitag,[37] Marie-Laure Jullié,[38] Julien Haroche,[39] Matthew Collin,[40] Jackie Allotey,[41] Majid Madni,[42] Kerry Turner,[43] Susan Picton,[44] Pasquale M. Barbaro,[45] Alysa Poulin,[46] Ingrid S. Tam,[46] Dina El Demellawy,[47] Brianna Empringham,[48] James A. Whitlock,[48] Aditya Raghunathan,[49] Amy A. Swanson,[49] Mariko Suchi,[50] Jon M. Brandt,[51] Nabeel R. Yaseen,[52] Joanna L. Weinstein,[53] Irem Eldem,[54] Bryan A. Sisk,[54] Vaishnavi Sridhar,[55] Mandy Atkinson,[55] Lucas R. Massoth,[56] Jason L. Hornick,[57] Sanda Alexandrescu,[57,58] Kee Kiat Yeo,[59] Kseniya Petrova-Drus,[5] Stephen Z. Peeke,[60] Laura S. Muñoz-Arcos,[61] Daniel G. Leino,[3] David D. Grier,[3] Robert Lorsbach,[3] Somak Roy,[3] Ashish R. Kumar,[62,63] Shipra Garg,[64] Nishant Tiwari,[64] Kristian T. Schafernak,[64] Michael M. Henry,[65] Astrid G. S. van Halteren,[2,66] Oussama Abla,[48] Eli L. Diamond,[67,†] and Jean-François Emile[6,7,†]

[1]Department of Pathology, Leiden University Medical Center, Leiden, The Netherlands; [2]Princess Máxima Center for Pediatric Oncology, Utrecht, The Netherlands; [3]Division of Pathology, Cincinnati Children's Hospital Medical Center, Cincinnati, OH; [4]Human Oncology and Pathogenesis Program, Department of Medicine, and [5]Department of Pathology, Memorial Sloan-Kettering Cancer Center, New York, NY; [6]Department of Pathology, Ambroise Paré Hospital, Assistance Publique–Hôpitaux de Paris, Boulogne, France; [7]EA4340-Biomarqueurs et Essais Cliniques en Cancérologie et Onco-Hématologie, Versailles Saint-Quentin-en-Yvelines University, Boulogne, France; [8]Department of Pediatric Oncology, Emma Children's Hospital, and [9]Department of Pathology, Amsterdam University Medical Centers, Amsterdam, The Netherlands; [10]Department of Internal Medicine and Immunology, and [11]Section of Clinical Immunology, Department of Immunology, and [12]Department of Pathology, Erasmus Medical Center University Medical Center Rotterdam, Rotterdam, The Netherlands; [13]Department of Pathology, Radboud University Medical Center, Nijmegen, The Netherlands; [14]Department of General Medical Oncology, University Hospitals Leuven, Leuven Cancer Institute, Leuven, Belgium; [15]Department of Pathology, University Hospitals Leuven, Katholieke Universiteit Leuven, Leuven, Belgium; [16]Department of Pediatric Hematology and Oncology, and [17]Department of Pathology, Hannover Medical School, Hannover, Germany; [18]Department I – General Pediatrics, Children's Hospital, Hematology and Oncology, [19]Department of Hematology and Oncology, and [20]Department of Pathology and Neuropathology and Comprehensive Cancer Center, University Hospital Tuebingen, Tuebingen, Germany; [21]Department of Oncology, Hematology and Stem Cell Transplantation, University Children's Hospital Würzburg, Würzburg, Germany; [22]Department of Pathology, University of Würzburg and Comprehensive Cancer Center Mainfranken, Würzburg, Germany; [23]Division of Pediatric Hematology and Oncology, Department of Pediatrics, Klinikum Chemnitz, Chemnitz, Germany; [24]Department of Oncology, Children's Memorial Health Institute, Warsaw, Poland; [25]Dmitriy Rogachev National Center for Pediatric Hematology, Oncology and Immunology, Moscow, Russia; [26]Department of Hematology and Oncology, Municipal Educational Hospital N°31, Saint Petersburg, Russia; [27]Department of Bone Marrow Transplantation and [28]Department of Pathology, Pavlov First Saint Petersburg State Medical University, Saint Petersburg, Russia; [29]Department of Hematology/Oncology, Cell and Gene Therapy, Bambino Gesù Children's Hospital Istituto di Ricovero e Cura a Carattere Scientifico (IRCCS), Rome, Italy; [30]Pathology Unit, Laboratories Department, Bambino Gesù Children's Hospital IRCCS, Rome, Italy; [31]Department of Pathology and [32]Department of Pediatric Neurosurgery, Fondazione Policlinico Universitario A. Gemelli IRCCS, Rome, Italy; [33]Department of Pediatric Hematology and Oncology, Trousseau Hospital, Assistance Publique-Hôpitaux de Paris, Paris, France; [34]Department of Pediatric Onco-Hematology and [35]Department of Pathology, Rennes University Hospital, Rennes, France; [36]Department of Hematology, La Conception, University Hospital of Marseille, Marseille, France; [37]Department of Pathology, Necker-Enfants Malades Hospital, Assistance Publique–Hôpitaux de Paris, Paris, France; [38]Department of Pathology, University Hospital of Bordeaux, Bordeaux, France; [39]Department of Internal Medicine, University Hospital La Pitié-Salpêtrière Paris, French National Reference Center for Histiocytoses, Assistance Publique–Hôpitaux de Paris, Paris, France; [40]Newcastle upon Tyne Hospitals, Newcastle upon Tyne, United Kingdom; [41]Department of Pathology and [42]Department of Pediatric Hematology and Oncology, Nottingham University Hospitals, Nottingham, United Kingdom; [43]Department of Histopathology and [44]Department of Pediatric Oncology, Leeds Children's Hospital, Leeds, United Kingdom; [45]Department of Hematology, Queensland Children's Hospital, Brisbane, QLD, Australia; [46]Department of Pathology and Laboratory Medicine, University of Saskatchewan, Saskatoon, SK, Canada; [47]Department of Pathology, Children's Hospital of Eastern Ontario, Ottawa, ON, Canada; [48]Department of Hematology/Oncology, The Hospital for Sick Children, University of Toronto, Toronto, ON, Canada; [49]Division of Anatomic Pathology, Mayo Clinic Rochester, Rochester, MN; [50]Department of Pathology, Medical College of Wisconsin, Milwaukee, WI; [51]Department of Pediatric Oncology, Hospital Sisters Health System St Vincent Children's Hospital, Green Bay, WI; [52]Department of Pathology, Northwestern University Feinberg School of Medicine, Chicago, IL; [53]Department of Hematology, Oncology and Stem Cell Transplantation, Ann & Robert H. Lurie Children's Hospital of Chicago, Northwestern University Feinberg School of Medicine, Chicago, IL; [54]Department of Pediatric Hematology and Oncology, St Louis Children's Hospital, Washington University in St Louis, St Louis, MO; [55]Department of Pediatric Hematology and Oncology, Carilion Children's Pediatric Hematology and Oncology, Roanoke, VA; [56]Department of Pathology, Massachusetts General Hospital, and [57]Department of Pathology, Brigham and Women's Hospital, Harvard Medical School, Boston, MA; [58]Department of Pathology, Boston Children's Hospital, Boston, MA; [59]Department of Pediatric Oncology, Dana Farber/Boston Children's Cancer and Blood Disorders Center, Boston, MA; [60]Department of Hematology and

Medical Oncology, Maimonides Medical Center, Brooklyn, NY; [61]Department of Internal Medicine, Montefiore Medical Center, Albert Einstein College of Medicine, Bronx, NY; [62]Department of Pediatrics, University of Cincinnati College of Medicine, Cincinnati, OH; [63]Division of Bone Marrow Transplantation and Immune Deficiency, Cincinnati Children's Hospital Medical Center, Cincinnati, OH; [64]Department of Pathology and [65]Center for Cancer and Blood Disorders, Phoenix Children's Hospital, Phoenix, AZ; [66]Department of Pediatrics, Leiden University Medical Center, Leiden, The Netherlands; and [67]Department of Neurology, Memorial Sloan-Kettering Cancer Center, New York, NY

KEY POINTS

- **ALK-positive histiocytosis is a distinct entity associated with *KIF5B-ALK* fusions and characterized by frequent neurologic involvement.**
- **ALK inhibition induces robust and durable responses in patients with ALK-positive histiocytosis.**

ALK-positive histiocytosis is a rare subtype of histiocytic neoplasm first described in 2008 in 3 infants with multisystemic disease involving the liver and hematopoietic system. This entity has subsequently been documented in case reports and series to occupy a wider clinicopathologic spectrum with recurrent *KIF5B-ALK* fusions. The full clinicopathologic and molecular spectra of ALK-positive histiocytosis remain, however, poorly characterized. Here, we describe the largest study of ALK-positive histiocytosis to date, with detailed clinicopathologic data of 39 cases, including 37 cases with confirmed *ALK* rearrangements. The clinical spectrum comprised distinct clinical phenotypic groups: infants with multisystemic disease with liver and hematopoietic involvement, as originally described (Group 1A: 6/39), other patients with multisystemic disease (Group 1B: 10/39), and patients with single-system disease (Group 2: 23/39). Nineteen patients of the entire cohort (49%) had neurologic involvement (7 and 12 from Groups 1B and 2, respectively). Histology included classic xanthogranuloma features in almost one-third of cases, whereas the majority displayed a more densely cellular, monomorphic appearance without lipidized histiocytes but sometimes more spindled or epithelioid morphology. Neoplastic histiocytes were positive for macrophage markers and often conferred strong expression of phosphorylated extracellular signal-regulated kinase, confirming MAPK pathway activation. *KIF5B-ALK* fusions were detected in 27 patients, whereas *CLTC-ALK, TPM3-ALK, TFG-ALK, EML4-ALK,* and *DCTN1-ALK* fusions were identified in single cases. Robust and durable responses were observed in 11/11 patients treated with ALK inhibition, 10 with neurologic involvement. This study presents the existing clinicopathologic and molecular landscape of ALK-positive histiocytosis and provides guidance for the clinical management of this emerging histiocytic entity.

Introduction

Histiocytic disorders are a group of rare diseases characterized by the accumulation of macrophage-, dendritic cell–, or monocyte-differentiated cells in various tissues and organs.[1,2] With the advent of molecular technologies, recurrent genetic alterations have been identified in several histiocytoses,[3-17] reframing the conceptualization of these disorders from one of primary inflammatory conditions to that of clonal neoplastic diseases.[18,19] These alterations primarily affect genes encoding protein kinases of the intracellular mitogen-activated protein kinase (MAPK) signaling pathway, leading to constitutive activation of this pathway (Figure 1).[11] However, downstream extracellular signal-regulated kinase (ERK) activation has also been observed in histiocytoses without detected MAPK pathway mutations,[3,11,13] leading to the notion that histiocytic neoplasms are uniformly characterized by dependence on MAPK signaling.[20] This has led to the clinical implementation of pharmacological inhibitors of the MAPK signaling pathway (BRAF and/or MEK inhibitors) for the treatment of patients with severe and/or relapsed/refractory histiocytic disease.[20-27] In addition to MAPK pathway mutations, recurrent activating genetic alterations in genes encoding protein kinases of the PI3K/AKT/mTOR signaling pathway (ie, *PIK3CA*) or receptor tyrosine kinases (ie, *CSF1R, NTRK1, RET,* or *ALK*) have been identified in a subset of histiocytic neoplasms.[6,13] Furthermore, significant associations between specific kinase alterations and clinicopathologic phenotypes have recently been observed.[6] These findings pave the way for molecular (sub)-classification of histiocytic neoplasms,[1,6,8,28] and highlight the potential for targeted therapy beyond BRAF or MEK inhibition in histiocytosis patients.

In 2008, Chan et al first described 3 infants with a novel type of systemic histiocytosis characterized by ALK immunoreactivity in large CD163$^+$ histiocytes with variable expression of other histiocyte/dendritic cell markers (S100, fascin, factor XIIIa).[29] Clinically, the disease was characterized by liver and hematopoietic involvement and could be confused with a storage disorder or leukemia. The disease tended to resolve slowly, sometimes even without any specific treatment but only supportive care. One case demonstrated a *TPM3-ALK* translocation. Over the following years, several individual case reports and small case series about ALK$^+$ histiocytosis have been published,[30-49] confirming the rare but indefinite occurrence of this emerging histiocytic entity. Most notably, Chang et al described a series of 10 cases,[43] including the original 3 cases reported by Chan et al, with 8 having molecular confirmation of *ALK* rearrangements. Together, these reports have documented ALK-positive histiocytosis in both older children and adults with single- or multisystemic disease, expanding beyond the initial observation of the disease as a systemic disorder of infancy. Moreover, the frequent presence of *KIF5B-ALK* fusions has been reported,[43] and successful treatment of some patients with ALK inhibition has been described.[6,27,33,34,39,40,43,50,51] Due to the modest number of reported patients, and particularly few cases with clinical information and/or successful molecular analysis, the full clinicopathologic and molecular spectra of ALK-

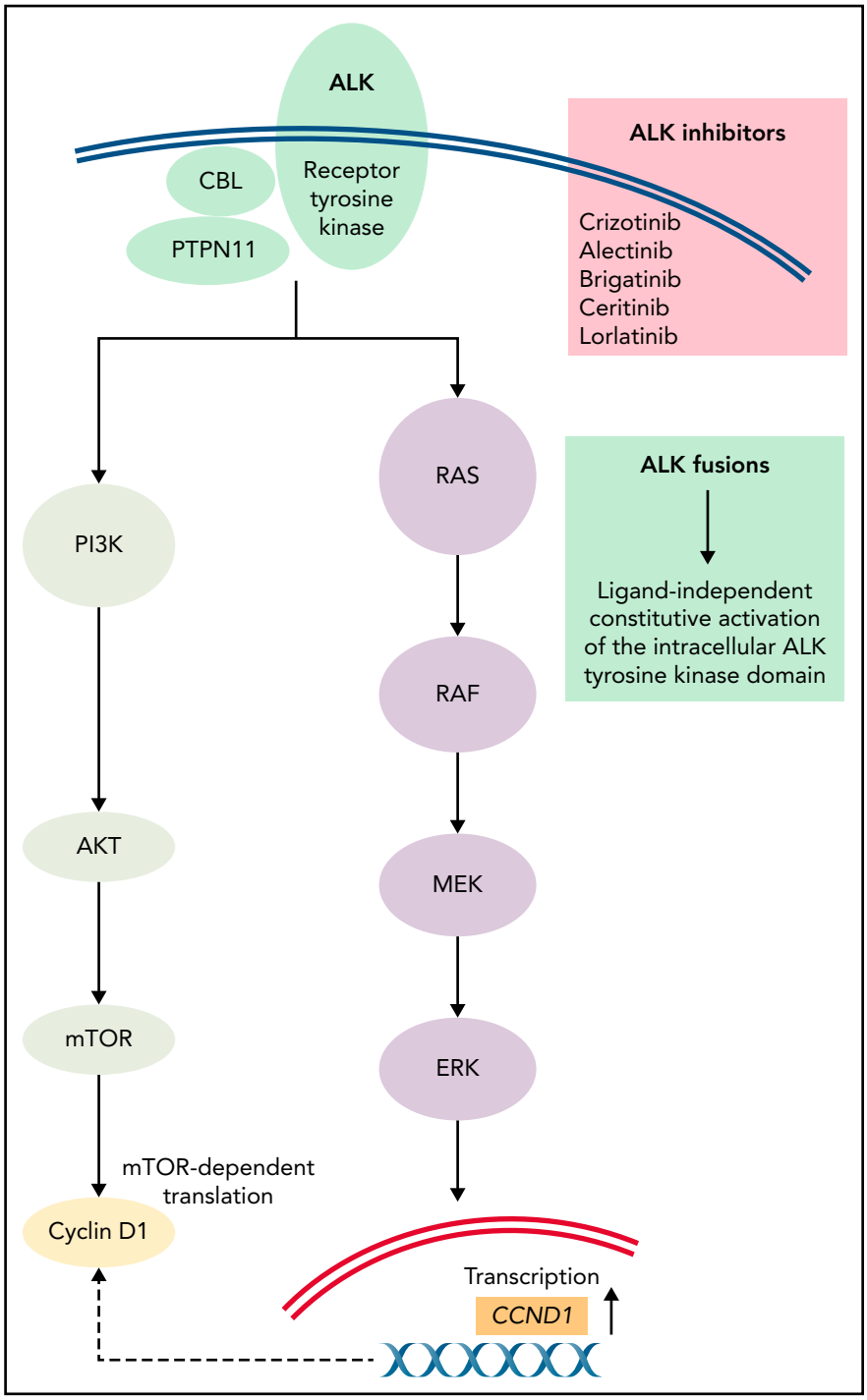

Figure 1. Schematic overview of downstream ALK signaling through MAPK and PI3K/AKT/mTOR signaling pathways. ALK is a classical receptor tyrosine kinase consisting of an extracellular ligand-binding domain, a transmembrane domain, and an intracellular tyrosine kinase domain.[76] In *ALK* fusions such as *KIF5B-ALK*, the amino-terminal fusion partner is fused to the intracellular tyrosine kinase domain of ALK, leading to constitutive activation of downstream signaling, including RAS-RAF-MEK-ERK (MAPK) and PI3K/AKT/mTOR signaling pathways. MAPK pathway activation ultimately leads to phosphorylation of downstream ERK, which can enter the nucleus and increase the transcription of various effector genes, including the gene encoding for Cyclin D1 (*CCND1*). Translation of *CCND1* messenger RNA to the Cyclin D1 protein is mTOR-dependent.[77] Figure adapted from Emile et al,[2] with permission from the authors.

positive histiocytosis remain, however, incompletely characterized. Accordingly, here we describe the results of the largest study of ALK-positive histiocytosis to date, outlining the clinicopathologic features of 39 patients, including 37 cases with proven *ALK* rearrangements.

Materials and methods

Patient selection and confirmation of diagnosis

Fifty-two cases from different hospitals throughout North America, Europe, and Australia were compiled for this international retrospective study. Six cases were previously published[6,30,31,39,44,47]

Table 1. Clinical and molecular characteristics of the distinct clinical phenotypic groups of ALK-positive histiocytosis and the overall cohort

	Group 1A (n = 6)	Group 1B (n = 10)	Group 2 (n = 23)	Overall (n = 39)
Age at presentation				
Median age (range)	1.5 mo (0-5 mo)	14.5 y (0-41 y)	7 y (0-41 y)	3 y (0-41 y)
Child	6 (100%)	5 (50%)	20 (87%)	31 (79%)
Adult		5 (50%)	3 (13%)	8 (21%)
Sex				
Female	4 (67%)	7 (70%)	13 (57%)	24 (62%)
Male	2 (33%)	3 (30%)	10 (43%)	15 (38%)
Organ involvement				
Nervous system		7 (70%)	12 (52%)	19 (49%)
Liver	6 (100%)	5 (50%)		11 (28%)
Lung	1 (17%)	7 (70%)	1 (4%)	9 (23%)
Bone		7 (70%)	2 (9%)	9 (23%)
Skin	1 (17%)	4 (40%)	4 (17%)	9 (23%)
Soft tissue		3 (30%)	4 (17%)	7 (18%)
Hematopoietic system	6 (100%)			6 (15%)
Spleen	5 (83%)			5 (13%)
Kidney	2 (33%)	2 (20%)		4 (10%)
Lymph node		4 (40%)		4 (10%)
Breast		2 (20%)		2 (5%)
Pancreas		2 (20%)		2 (5%)
Other*		2 (20%)		2 (5%)
***ALK* rearrangement**				
KIF5B-ALK	1 (17%)	7 (70%)	19 (83%)	27 (69%)
CLTC-ALK	1 (17%)			1 (3%)
TPM3-ALK		1 (10%)		1 (3%)
TFG-ALK		1 (10%)		1 (3%)
EML4-ALK			1 (4%)	1 (3%)
DCTN1-ALK			1 (4%)	1 (3%)
ALK-FISH+	2 (33%)	1 (10%)	2 (9%)	5 (13%)
Not confirmed	2 (33%)			2 (5%)
Median follow-up (range)	3.75 y (0-7 y)	2 y (0-6 y)	14 mo (0-18 y)	21 mo (0-18 y)
Status at last follow-up				
Alive with				
no evidence of disease	4 (67%)	5 (50%)	14 (61%)	23 (59%)
regressive disease		4 (40%)	5 (22%)	9 (23%)
stable disease			1 (4%)	1 (3%)
recent diagnosis			1 (4%)	1 (3%)
Dead	1 (17%)	1 (10%)		2 (5%)
Lost to follow-up	1 (17%)		2 (9%)	3 (8%)

*Cervix, thyroid, salivary glands, and colorectum.

Table 2. Treatments and outcomes of the different clinical groups of ALK-positive histiocytosis and the overall cohort

	Group 1A (n = 6)			Group 1B (n = 10)			Group 2 (n = 23)			Overall (n = 39)		
	Number of cases	Objective response	Progression or relapse	Number of cases	Objective response	Progression or relapse	Number of cases	Objective response	Progression or relapse	Number of cases	Objective response	Progression or relapse
First-line												
Conventional systemic therapy	3 (50%)	1/3 (33%)	3/3 (100%)	6 (60%)	3/6 (50%)	2/6 (33%)	4 (17%)†	3/4 (75%)	1/4 (25%)	13 (33%)	7/13 (54%)	6/13 (46%)
Surgical resection							13 (57%)‡	11/13 (85%)	2/13 (15%)	13 (33%)	11/13 (85%)	2/13 (15%)
ALK inhibition				4 (40%)*	4/4 (100%)	0/4 (0%)	1 (4%)	1/1 (100%)	0/1 (0%)	5 (13%)	5/5 (100%)	0/5 (0%)
Observation & supportive care	2 (33%)	2/2 (100%)	0/2 (0%)				1 (4%)	1/1 (100%)	0/1 (0%)	3 (8%)	3/3 (100%)	0/3 (0%)
Radiotherapy							1 (4%)	1/1 (100%)	0/1 (0%)	1 (3%)	1/1 (100%)	0/1 (0%)
Unknown or not treated yet	1 (17%)						3 (13%)			4 (10%)		
Second- and further-line												
ALK inhibition				3 (30%)	3/3 (100%)	0/3 (0%)	3 (13%)	3/3 (100%)	0/3 (0%)	6 (15%)	6/6 (100%)	0/6 (0%)
Conventional systemic therapy	3 (50%)	2/3 (67%)	1/3 (33%)				2 (9%)	0/2 (0%)	2/2 (100%)	5 (13%)	2/5 (40%)	3/5 (60%)

*Including 2 patients treated with a combination of ALK inhibition and chemotherapy.

†Including 2 patients treated with chemotherapy following surgical resection.

‡Including 2 patients who received systemic corticosteroids before surgical resection.

Table 3. Individual patient data of cases with ALK-positive histiocytosis (n = 39) or atypical *ALK*-rearranged histiocyte-rich tumors (n = 3)

No.	Gene fusion	Sex	Age*	Sites of disease	First-line treatment	Response	Progression /relapse	Second- and further-line treatment	Last response	Therapy ongoing	Outcome (follow-up†)
Group 1A: infants with multistemic disease with liver and hematopoietic involvement											
1‡	N/A	F	0 d	Liver, hematopoietic system, spleen, lung, possibly kidney	IVIG (2 d), corticosteroids (tapered after diagnosis), and supportive care (transfusions)	CR	No	—	—	No	Alive with no disease (3.5 y)
2‡	*ALK-FISH+*	F	27 d	Liver, hematopoietic system, spleen, + kidney at relapse	Chemotherapy (VBL/ PRED, 6 mo)	PR	Yes	Chemotherapy	CR	No	Alive with no disease (7 y)§
3	*KIF5B-ALK*	M	1 mo	Liver, hematopoietic system, spleen, kidney, skin	Chemotherapy (VBL/ DEX/MTX, 3 wk)	PD	Yes	Chemotherapy (2-CDA, 1 wk)	PD	No	Died of coagulopathy and sepsis (1 mo)
4	N/A	F	2 mo	Liver, hematopoietic system, spleen	Supportive care (transfusions)	CR	No	—	—	No	Alive with no disease (4.5 y)
5	*ALK-FISH+*	F	4 mo	Liver, hematopoietic system	N/A	N/A	N/A	N/A	N/A	N/A	N/A (lost to follow-up)
6	*CLTC-ALK*	M	5 mo	Liver, hematopoietic system, spleen	Corticosteroids (PRED 40mg/m2, 2.5 wk), followed by chemotherapy (VBL + tapered PRED, 2.5 wk)	PD	Yes	Dexamethasone + anakinra (1 mo), followed by anakinra (3 mo) + azathioprine (4.5 mo)	CR	No	Alive with no disease (4 y)
Group 1B: other patients with multisystemic disease											
7	*TPM3-ALK*	F	3 mo	Bone, lung, liver	Chemotherapy (VBL/ PRED/6MP, 18 mo)	CR	No	—	—	No	Alive with no disease (2 y)
8	*ALK*-FISH+	F	9 mo	Lung, skin, kidney	Chemotherapy (VBL/ PRED, 12 mo)	CR	No	—	—	No	Alive with no disease (2 y)
9‡	*KIF5B-ALK*	M	10 mo	CNS, lung, liver, soft tissue (peritoneum)	Chemotherapy (VBL/ PRED), combined with ALK inhibition (alectinib)	CR	No	—	—	Yes (VBL/ PRED + alectinib)	Alive with no disease (13 mo)
10	*KIF5B-ALK*	F	2 y	CNS, bone, lung, liver, skin, soft tissue (perineal mass), lymph node, kidney, breast, pancreas	Chemotherapy (VBL/ PRED, 6 wk induction)	SD	No	ALK inhibition (lorlatinib)	PR	Yes (lorlatinib)	Alive with regressive disease (21 mo)

Table 3. (continued)

No.	Gene fusion	Sex	Age*	Sites of disease	First-line treatment	Response	Progression /relapse	Second- and further-line treatment	Last response	Therapy ongoing	Outcome (follow-up†)
11	*KIF5B-ALK*	F	10 y	CNS, bone, lung, lymph node, cervix, thyroid, submandibular salivary gland	ALK inhibition (crizotinib)	CR	No	—	—	Yes (crizotinib)	Alive with no disease (2 y)
12	*KIF5B-ALK*	F	19 y	CNS/PNS, bone, lung, liver, lymph node, breast, pancreas	Chemotherapy (2-CDA, 3 cycles), followed by ALK inhibition (alectinib)	PR	No	—	—	Yes (alectinib)	Alive with stable ($PET^{negative}$) bone lesions on MRI; other lesions regressed (2 y)
13	*TFG-ALK*	M	21 y	Liver, skin, colorectum	Corticosteroids (high-dose)	PR	Yes‖	—	—	No	Died of sepsis (2 mo)
14	*KIF5B-ALK*	F	28 y	CNS/PNS, bone	ALK inhibition (alectinib)	PR	No	—	—	Yes (alectinib)	Alive with regressive ($PET^{negative}$) disease (9 mo)
15	*KIF5B-ALK*	M	29 y	PNS (incl. cerebrospinal fluid pleocytosis), bone	Corticosteroids, followed by pegylated interferon-α (with escalation to 180μg/wk, 4 mo)	SD	No	ALK inhibition (brigatinib)	CR	Yes (brigatinib)	Alive with no disease (2.5 y)
16‡	*KIF5B-ALK*	F	41 y	CNS, bone, lung, skin, soft tissue (omentum/peritoneum), lymph node	Interferon-α (16 mo)	PD	Yes	ALK inhibition (crizotinib)	PR	Yes (crizotinib)	Alive with regressive disease (6 y)
Group 2: single-system neurologic disease											
17	*KIF5B-ALK*	F	7 mo	CNS: thalamus	Corticosteroids, followed by ALK inhibition (lorlatinib)	PR	No	—	—	Yes (lorlatinib)	Alive with regressive disease (5 mo)
18	*ALK*-FISH+	F	9 mo	CNS: cerebellum	N/A	N/A	N/A	N/A	N/A	N/A	N/A (lost to follow-up)
19	*KIF5B-ALK*	M	2.5 y	CNS: right medulla tumor extending through the foramen of Luschka	Chemotherapy (Headstart protocol, 1 cycle)	PD	Yes	ALK inhibition (alectinib)	CR	Yes (alectinib)	Alive with no disease (16 mo)
20	*KIF5B-ALK*	F	3 y	CNS: cerebellum, cranial nerves, spinal cord, cerebrospinal fluid	Corticosteroids, followed by surgery (subtotal resection cerebellar tumor)	CR	No	—	—	No	Alive with no disease (12 mo)

Table 3. (continued)

No.	Gene fusion	Sex	Age*	Sites of disease	First-line treatment	Response	Progression /relapse	Second- and further-line treatment	Last response	Therapy ongoing	Outcome (follow-up†)
21	*KIF5B-ALK*	F	3 y	PNS: left oculomotor nerve with extraneural extension	Corticosteroids, followed by surgery (subtotal resection) and chemotherapy (VBL/PRED, 6 mo)	PR	No	—	—	No	Alive with mildly regressive disease (2.5 y)
22	*KIF5B-ALK*	F	7 y	CNS: left medulla	Chemotherapy (Clofarabine, 6 cycles)	CR	No	—	—	No	Alive with no disease (6 mo)
23‡	*KIF5B-ALK*	F	11 y	CNS: right frontal lobe	Surgery (total resection)	CR	No	—	—	No	Alive with no disease (9 mo)
24	*ALK*-FISH+	M	11 y	PNS: left trigeminal nerve	Surgery (subtotal resection)	CR	No	—	—	No	Alive with no disease (18 y)
25	*KIF5B-ALK*	M	12 y	PNS: intradural extramedullary tumor at level C1-C2	Surgery (total resection), followed by chemotherapy (VBL/PRED, 12 mo)	CR	No	—	—	No	Alive with no disease (2.5 y)
26	*KIF5B-ALK*	F	13 y	CNS/PNS: left insula, cranial & spinal nerves, pituitary stalk, + cerebrospinal fluid at relapse	Surgery (subtotal resection insula tumor)	PD	Yes	ALK inhibition (alectinib)	PR	Yes (alectinib)	Alive with minor, regressive disease (2.5 y)
27	*KIF5B-ALK*	M	20 y	PNS: 3 intradural extramedullary lesions at levels L3 and S1	Not treated yet	Not yet evaluable	Not yet evaluable	—	—	No	Alive with active disease (7 mo)
28	*KIF5B-ALK*	M	20 y	CNS: right frontal lobe	Surgery (total resection)	CR	No	—	—	No	Alive with no disease (10 mo)
Group 2: single-system nonneurologic disease											
29	*KIF5B-ALK*	F	6 mo	Skin: retroauricular scalp lesion	Active monitoring (4 mo), followed by surgery (subtotal resection)	CR	No	—	—	No	Alive with no disease (2 y)
30	*KIF5B-ALK*	M	7 mo	Skin: papular lesion on the back	Surgery (total resection)	CR	No	—	—	No	Alive with no disease (13 mo)
31	*KIF5B-ALK*	F	21 mo	Skin: midline posterior scalp lesion	Surgery (total resection)	CR	No	—	—	No	Alive with no disease (2 y)

Table 3. (continued)

No.	Gene fusion	Sex	Age*	Sites of disease	First-line treatment	Response	Progression /relapse	Second- and further-line treatment	Last response	Therapy ongoing	Outcome (follow-up†)
32	*KIF5B-ALK*	M	2 y	Soft tissue: subcutaneous tumor left lower leg with infiltration in the musculature	Active monitoring	PR	No	—	—	No	Alive with regressive disease (14 mo)
33	*KIF5B-ALK*	F	3 y	Soft tissue: perineal mass	Surgery (total resection)	CR	No	—	—	No	Alive with no disease (14 mo)
34‡	*KIF5B-ALK*	M	3 y	Soft tissue: subglottic mass	Corticosteroids, followed by surgery (total resection)	CR	No	—	—	No	Alive with no disease (3 y)
35	*KIF5B-ALK*	F	10 y	Skin: single nodule on the right breast (7mm; exclusively dermal/ cutaneous)	Surgery (total resection)	CR	No	—	—	No	Alive with no disease (1 mo)
36	*KIF5B-ALK*	F	10 y	Bone: right scapular lesion with soft tissue extension	Surgery (total resection)	CR	No	—	—	No	Alive with no disease (5 y)
37	*KIF5B-ALK*	M	11 y	Soft tissue: 2 tumors in omentum and mesenterium	Surgery (subtotal resection)	PD	Yes	Chemotherapy (VBL/ PRED, 12 wk, IC-1/ IC-2, → PD), followed by active monitoring¶	SD	No	Alive with stable disease (15 mo)
38	*EML4-ALK*	M	17 y	Lung: single mass (10 × 9 × 8 cm) within the left lower lobe extending into the pulmonary vein and left atrium	N/A	N/A	N/A	N/A	N/A	N/A	N/A (lost to follow-up)
39	*DCTN1-ALK*	F	41 y	Bone: right clavicular lesion with significant soft tissue extension (total size >10 cm)	Radiotherapy (22 Gy in 12 fractions)	PR	No	ALK inhibition (crizotinib → severe anaphylaxis), followed by chemotherapy (VBL/ PRED, 4 courses, → PD), and then ALK inhibition (alectinib)	PR	Yes (alectinib)	Alive with regressive disease (2 y)

Table 3. (continued)

No.	Gene fusion	Sex	Age*	Sites of disease	First-line treatment	Response	Progression /relapse	Second- and further-line treatment	Last response	Therapy ongoing	Outcome (follow-up†)
Atypical: *ALK*-rearranged histiocyte-rich tumors											
A1	*EML4-ALK*	F	51 y	CNS, bone, lung, + subcutaneous tumors at relapse	Surgery (L1 tumor), chemotherapy (TC, 1 cycle) and radiotherapy (32 Gy L1 tumor; 20 Gy whole brain)	PD	Yes	ALK inhibition (alectinib for 16 mo, followed by lorlatinib for 14 mo, and then ceritinib for 7 wk), followed by antalgic radiotherapy of 2 metastases and chemotherapy (VBL/PRED)	SD	Yes (VBL/Pred)	Alive with stable disease (3 y)
A2	*SQSTM1-ALK*	F	53 y	Soft tissue: large mesenteric tumor, + subcutaneous and liver tumors at relapse	Surgery (total resection)	PD	Yes	ALK inhibition (crizotinib)	SD	Yes (crizotinib)	Alive with stable disease (13 mo)
A3	*EML4-ALK*	F	4 y	Soft tissue: obstructing yellow nodule in the left main bronchus	Surgery (endoscopic resection)	N/A	Yes	Surgery (endoscopic reresection 1 and 2 y after first surgery)	CR	No	Alive with no disease (17 y)

2-CDA, cladribine; 6MP, mercaptopurine; CNS, central nervous system; CR, complete response; F, female; Gy, gray; IVIG, intravenous immunoglobulin; M, male; N/A, not available; PD, progressive disease; PNS, peripheral nervous system; PR, partial response; PRED, prednisone; SD, stable disease; TC, paclitaxel and cyclophosphamide; VBL, vinblastine.

*Age at presentation in hospital.

†Follow-up since presentation in hospital.

‡Previously reported cases (Case 1,[47] Case 2,[30,31] Case 9,[39] Case 16,[6] Case 23,[39] Case 34[44]).

§This patient experiences chronic renal insufficiency, hypertension, and hypergammaglobulinemia.

‖Death.

¶Abdominal MRI after chemotherapy demonstrated disease progression. Subsequent abdominal ultrasound exams at 2 and 4 mo after abdominal MRI showed stable disease; the patient has been asymptomatic since he received chemotherapy. Therefore, no second-line therapy was given at last follow-up, but active monitoring was executed. Active monitoring was performed using abdominal ultrasound because of significant distress of the child during MRI.

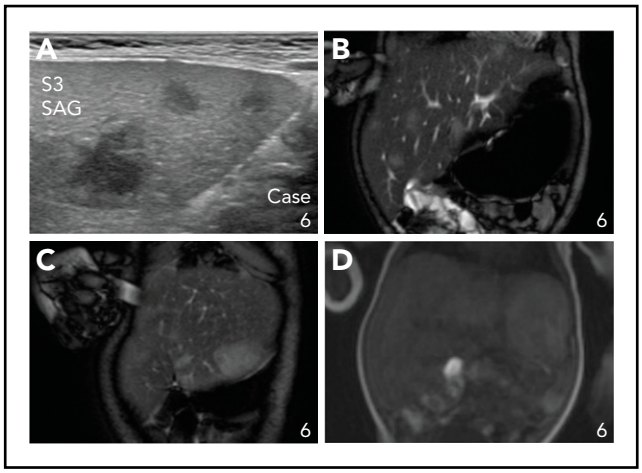

Figure 2. Focal liver lesions in an infant with multisystemic disease with liver and hematopoietic involvement (Group 1A). (A) Ultrasound image showing 3 hypoechoic lesions in liver segment 3. (B-C) Coronal T2-weighted fat-suppressed MRI images showing multiple hyperintense lesions in the liver, including a large rounded lesion in liver segment 3 (C). (D) Coronal T2-weighted contrast-enhanced MRI image showing late contrast accumulation in the large rounded lesion in liver segment 3.

and are reported with updated follow-up (when available). All cases underwent central review of pathology slides (J.P. and J.-F.E.) for confirmation of diagnosis. Additional immunohistochemical and/or molecular analyses were performed when deemed appropriate. Criteria for a diagnosis of ALK-positive histiocytosis and inclusion in the study were the following: (1) histologic confirmation of a histiocytosis,[1] with expression of at least 2 macrophage/histiocyte markers (including CD163, CD68, CD14, and/or CD4) by the lesional cells and (2A) molecular confirmation of *ALK* rearrangement and/or (2B) classic infantile systemic disease with diffuse strong ALK immunoreactivity as previously described.[29] Cases with *ALK* rearrangements in which immunohistochemistry revealed histiocytes to be disparate from lesional ALK^+ cells without immunoreactivity for macrophage/histiocyte markers were termed "atypical *ALK*-rearranged histiocyte-rich tumors" and not included in the primary study cohort. Also, histiocytosis cases with ALK immunoreactivity but without *ALK* rearrangements by comprehensive molecular analysis (ie, RNA sequencing [RNA-seq]) were not included in the primary study cohort. Cases excluded for these 2 reasons are characterized separately. Written informed consent for this study was obtained from the patients and/or their legal representative when required, or a waiver of consent was obtained from the relevant institutional review board for retrospective research.

Clinical and radiologic assessment and data collection

Clinical information was extracted from the medical records by the treating physicians and provided in a pseudonymized fashion according to a standardized deidentified case report form. Retrieved data included demographic characteristics, presenting symptoms, sites of disease involvement, treatments, and treatment outcomes. First- and second-or-further line treatments were categorized as observation with supportive care, surgical resection, radiotherapy, conventional systemic therapy (ie, cytotoxic chemotherapy, corticosteroids, immunosuppression, and/or interferon-α), ALK inhibition, or a combination of these. As previously published for Erdheim-Chester disease (ECD) and Langerhans cell histiocytosis (LCH),[27,52,53] responses to treatment as documented in the medical record were classified as complete response (complete resolution of disease), partial response (partial resolution of disease), stable disease (no significant change in lesions), or progressive disease (growth of known lesions or appearance of new lesions). Responses were extracted from the clinical medical records and based on formal clinical interpretations of ultrasound, computed tomography (CT), magnetic resonance imaging (MRI) and/or positron emission tomography (PET)-CT when available. The less favorable radiologic response was prioritized if multiple imaging methods were used that showed discrepant responses. Objective response was defined as partial or complete response. Whether or not progression or relapse of disease was subsequently observed was dichotomously captured. Progression was defined as progressive disease or death from any cause.

Histopathologic analysis

Histopathologic information was collected in a standardized deidentified case report form. Morphology and immunophenotype were reviewed for all cases (J.P. and J.-F.E.). Immunohistochemistry (IHC) was performed as part of initial diagnosis at participating institutions and consequently was executed using varying staining techniques and monoclonal antibodies. If ALK, CD163, CD68, S100, and/or CD1a IHC was not originally performed, these stains were done in the process of central review when sufficient tumor tissue was available. The ALK clones that were used for each case are shown in supplemental Table 1, available on the *Blood* Web site. The phosphorylated-ERK (*p*-ERK) immunostains were all performed using clone D13.14.4E (Cell Signaling).

Molecular pathologic analysis

Molecular pathologic information was collected in a standardized deidentified case report form. Molecular analysis was performed as part of initial diagnosis at referring institutions or done in the process of central review, when sufficient tumor tissue was available. For analyses performed during central review, fluorescence in situ hybridization (FISH) analysis was performed using CytoCell dual color ALK break-apart probes (Oxford Gene Technology) as previously described.[54] Targeted RNA-seq was performed using customized Archer FusionPlex next-generation sequencing (NGS) panels, which allow the detection of both fusions with known or unknown fusion partners. For NGS analysis at the European referral center Ambroise Paré Hospital (Paris, France), RNA was isolated using the Maxwell Rapid Sample Concentrator RNA Formalin-Fixed Paraffin-Embedded Kit (Promega), and RNA concentrations were measured using the Qubit RNA High Sensitivity Assay Kit (Thermo Fisher Scientific). Successful NGS required 20 to 250 ng RNA per reaction. Generated libraries were sequenced using a MiSeq system (Illumina), and produced reads were analyzed with Archer Analysis software. Archer RNA NGS at the North American referral center Memorial Sloan-Kettering Cancer Center (New York, NY) was performed as previously described.[55] Clonality assessment of T-cell receptor or immunoglobulin (Ig) gene rearrangements was performed using standardized multiplex polymerase chain reaction assays as previously described.[56,57]

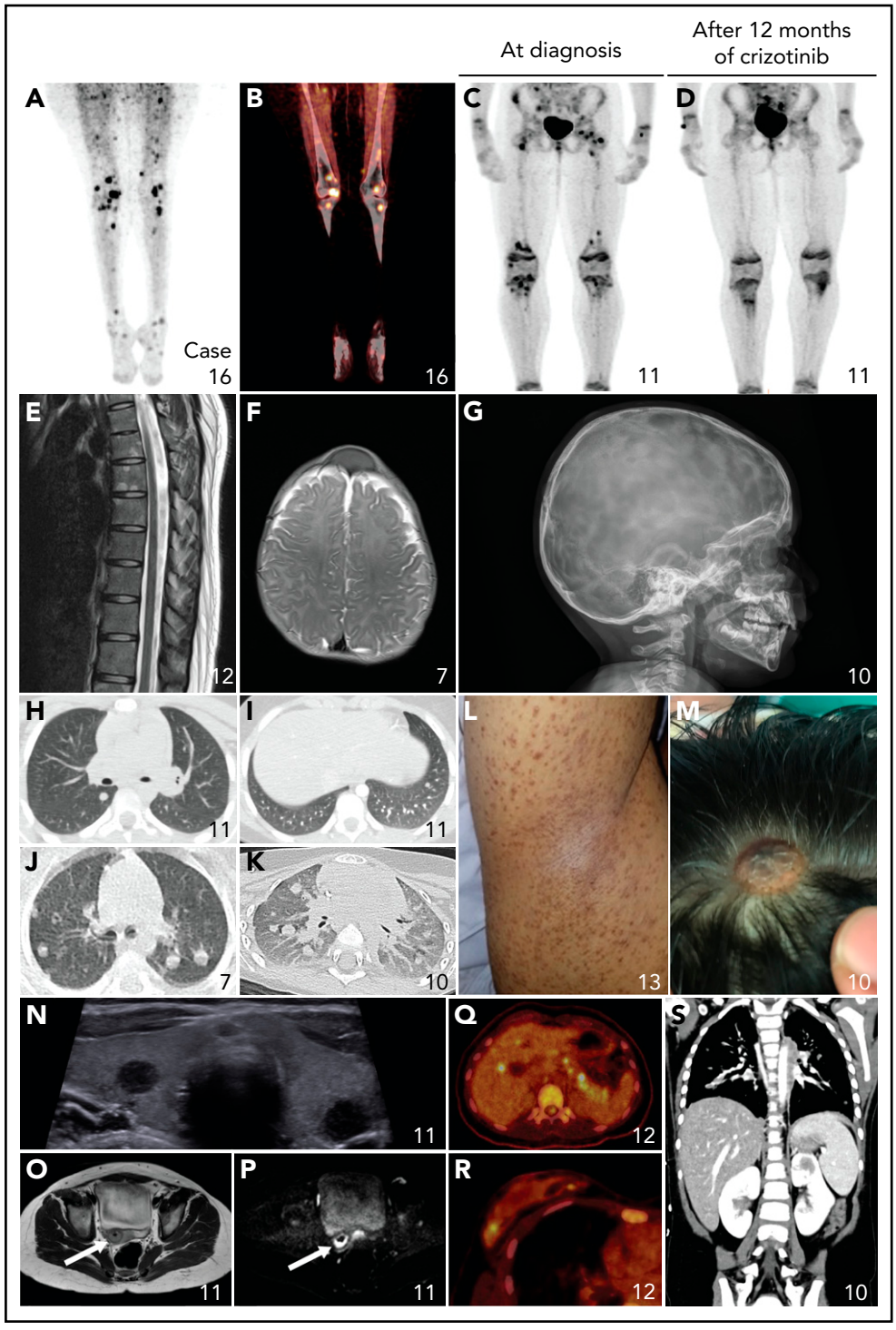

Figure 3. Nonneurologic disease manifestations in ALK-positive histiocytosis patients from Group 1B. (A-D) Fluorodeoxyglucose PET-CT images showing bilateral hypermetabolic long bone involvement, reminiscent of ECD, with objective metabolic response in Case 11 after 12 months of crizotinib. (E) Sagittal image of the contrast-enhanced MRI scan of the spine showing multiple hyperintense lesions in the vertebral bodies. (F-G) Axial MRI image (F) and lateral conventional radiograph (G) showing skull lesions in 2 children, with an appearance reminiscent of LCH. (H-K) Axial CT images showing nodular pulmonary involvement in 3 pediatric cases. (L) Photograph of the right axilla of an adult with a brown maculopapular exanthema that coalesces into plaques and predominates in the axillae and flanks, reminiscent of xanthoma disseminatum. (M) Photograph showing 1 of multiple scalp skin lesions in a child, which can also be observed on the MRI of the head (Figure 4A). (N) Ultrasound image demonstrating round, hypoechoic lesions in both lobes of the thyroid gland. (O-P) Axial T2-weighted (O) and diffusion-weighted (P) pelvic MRI images showing a cervical tumor with restricted diffusion in a child that presented with menorrhagia and irregular vaginal bleeding. (Q-R) Axial PET-CT images showing hypermetabolic focal lesions in the liver and pancreas (Q) and in the breast (R). (S) Coronal CT image showing a focal lesion in the left kidney.

Statistical analysis

Data were analyzed using descriptive statistics. Continuous variables were summarized with medians and ranges, and categorical variables were summarized with frequencies and proportions. Frequency of objective responses were summarized for treatment modality by patient group and for the entire cohort, and the frequency of disease progression or relapse following therapy was summarized.

Results

Thirty-nine patients meeting criteria for ALK-positive histiocytosis were identified and included in the study (Tables 1-3; supplemental Tables 1-3). In addition, 3 patients with atypical *ALK*-rearranged histiocyte-rich tumors were recognized (Table 3), and 10 patients were identified with histiocytoses demonstrating ALK immunoreactivity but no *ALK* rearrangement by RNA-seq (supplemental Table 4). These 13 patients without complete criteria for ALK-positive histiocytosis diagnosis were excluded from the primary study cohort and are described separately.

Clinical features

The 39 patients with ALK-positive histiocytosis comprised 24 females and 15 males and included 31 children and 8 adults (Table 1). Their age at presentation ranged from 0 days to 41 years: 1 infant had hepatosplenomegaly, anemia, and thrombocytopenia only 7 hours after birth.[47] Moreover, the 31 pediatric cases consisted of 21 children of 3 years or younger, including 13 infants (age $<$ 1 year). The 39 patients had diverse organ system manifestations (Figures 2-6) and were classified into 2 distinct clinical phenotypic groups: patients with multisystem disease (Group 1, n = 16) and patients with single-system disease (Group 2, n = 23). Within Group 1 were infants with systemic disease with liver and hematopoietic involvement as originally described[29] (Group 1A, n = 6) and other patients with multisystemic disease, not fitting the original infantile disease presentation (Group 1B, n = 10).

Infants with systemic disease with liver and hematopoietic involvement (Group 1A)

Patients in Group 1A ranged from 0 days to 5 months of age and presented with hepatomegaly, anemia, and thrombocytopenia. In addition, 5/6 had splenomegaly, 5/6 displayed leukocytosis, and some had measurable liver dysfunction, such as elevated liver enzymes, high bilirubin, and/or decreased serum protein and albumin levels. In 3 cases, focal lesions were seen in the liver (Figure 2). Coagulation profiles were available for 4/6 patients (supplemental Table 2), revealing prolonged prothrombin time, activated partial thromboplastin time, and decreased serum fibrinogen in Case 3. Small numbers of ALK$^+$ histiocytes were observed in the bone marrow of all 5 patients that had a bone marrow biopsy performed. Regarding additional sites of disease, 2/6 had renal involvement,[31] 1/6 had interstitial lung involvement requiring prolonged oxygen supplementation,[47] and 1/6 had skin involvement (Table 3).

Other patients with multisystemic disease (Group 1B)

Group 1B contained 5 children and 5 adults who presented with disseminated disease involving various organs (Table 1), including 3 infants without hematopoietic involvement. The most commonly involved organs were the nervous system (7/10), bone (7/10), lungs (7/10), liver (5/10), skin (4/10), and lymph nodes (4/10). All 3 pediatric cases with neurologic involvement had multiple masses in the brain (Figure 4A-E); adult cases had lesions of cranial and/or spinal nerves (3/4; Figure 4G-I), intramedullary spinal cord and/or leptomeningeal enhancement (2/4; Figure 4F), and/or parenchymal brain masses (1/4). Reminiscent of the localization of bone lesions in ECD, bone involvement included bilateral lesions in femora and/or tibiae in 7/7 patients (Figure 3A-D). Lung involvement was uniformly characterized by pulmonary nodules, ranging in size from micronodules to significant tumors (Figure 3H-K). All 5 patients with liver involvement had focal lesions on imaging.

Patients with single-system disease (Group 2)

Patients in Group 2 were 20 children and 3 adults, including 12 cases with neurologic involvement (52%). Patients with neurologic involvement presented with diverse neurological symptoms, including seizures (3/12), ataxia (3/12), headaches (3/12), vomiting (2/12), hypotonicity (2/12), unclear paroxysmal neurologic symptoms ("spells") (1/12), torticollis (1/12), trigeminal neuralgia (1/12), paresis (1/12), and diplopia (1/12). Tumoral lesions were widely distributed in the central and peripheral nervous system (Figure 4J-S; Table 3). In addition, 2 patients had cerebrospinal fluid monocytosis, including 1 case with a very low level of *ALK* rearrangements in the cerebrospinal fluid by FISH analysis. The 11 patients with non-neurologic disease comprised 1 case with a single lung tumor, 2 cases with solitary bone lesions, and 8 children with localized skin lesions or soft tissue tumors in varying locations (Figure 5; Table 3).

Treatments

Group 1A Two of 6 patients did not receive histiocytosis-directed therapy but were managed with supportive care including transfusions (Table 2). In both cases, spontaneous resolution of disease was observed. Three other patients were treated with chemotherapy. Two experienced progressive disease, including 1 patient that had worsening of ascites and died of coagulopathy and sepsis. The other received second-line systemic therapy with dexamethasone, anakinra, and azathioprine and obtained a complete response. The third patient achieved a partial response to first-line chemotherapy, relapsed with biopsy-proven renal involvement at 5 months after completion of treatment, and subsequently received a second round of chemotherapy.[31] The remaining patient was lost to follow-up.

Group 1B First-line therapy consisted of conventional systemic therapy alone in 6/10 patients and ALK inhibition with or without conventional therapy in 4/10 patients (Table 2). Conventional systemic therapy led to an objective response in 3/6 patients, 2 of whom had sustained complete responses to chemotherapy and 1 of whom died of (likely immunosuppression-related) sepsis following a partial response to high-dose corticosteroids (Table 3). The 3/6 patients with stable or progressive disease following conventional systemic therapy were treated with ALK inhibition as second-line therapy, with objective responses in all 3. ALK inhibition, with or without chemotherapy, led to an objective response in 4/4 patients in the first-line setting.

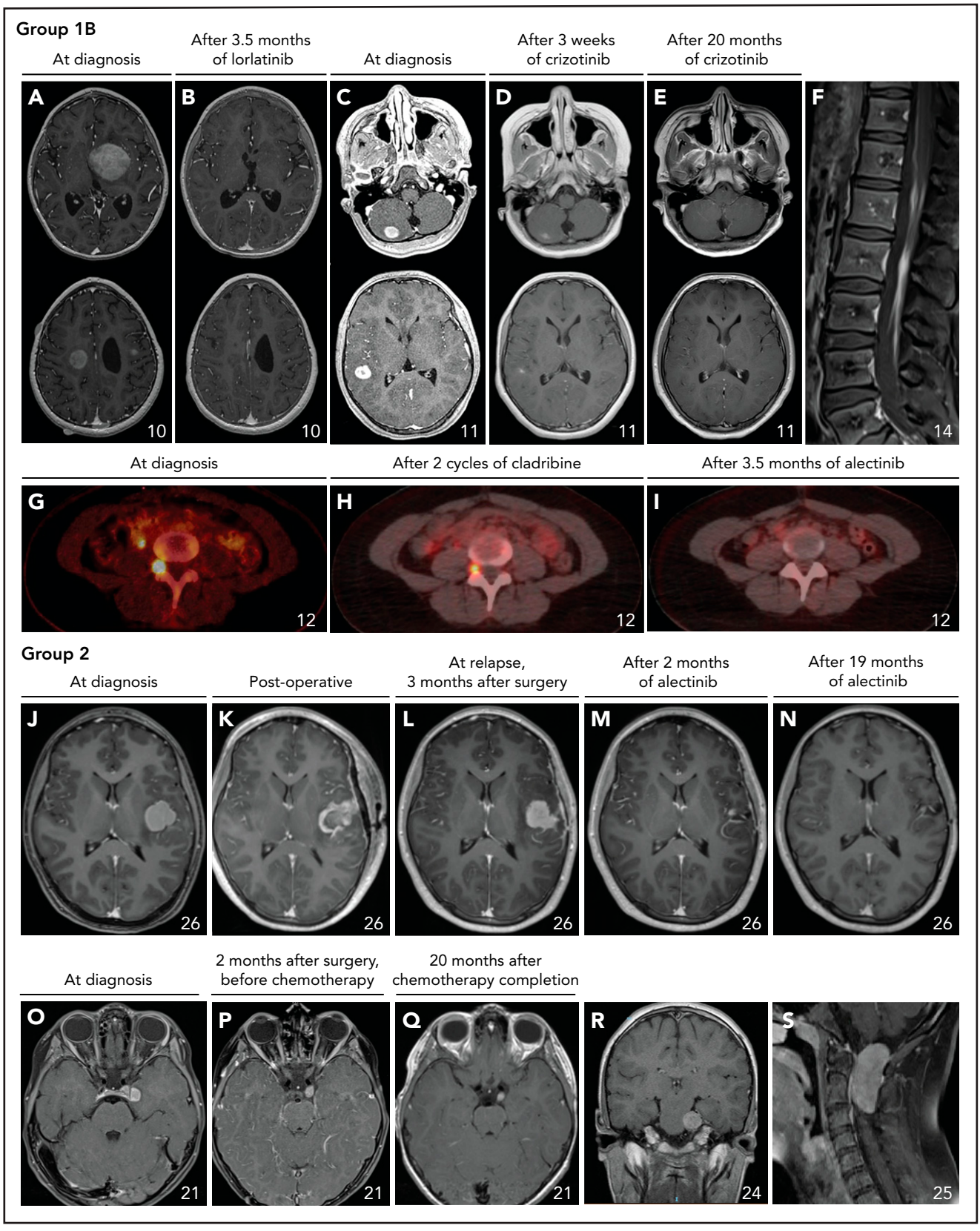

Figure 4. Neurologic involvement in ALK-positive histiocytosis patients from Group 1B or 2. (A-E) Axial images of the T1-weighted contrast-enhanced MRI scans of the heads of 2 pediatric cases with multiple solid brain tumors before and after treatment with ALK inhibition, demonstrating robust responses in both. (F) Sagittal image of the T1-weighted contrast-enhanced MRI scan of the spine showing leptomeningeal contrast enhancement along the descending cauda equina nerve roots. (G-I) Axial images of successive fluorodeoxyglucose PET-CT scans showing partial and complete response of a neuroforaminal tumor at level L5 after 2 cycles of cladribine (H) and subsequent treatment with alectinib (I), respectively. Coronal images (not shown) demonstrated that the tumor followed the course of the exiting

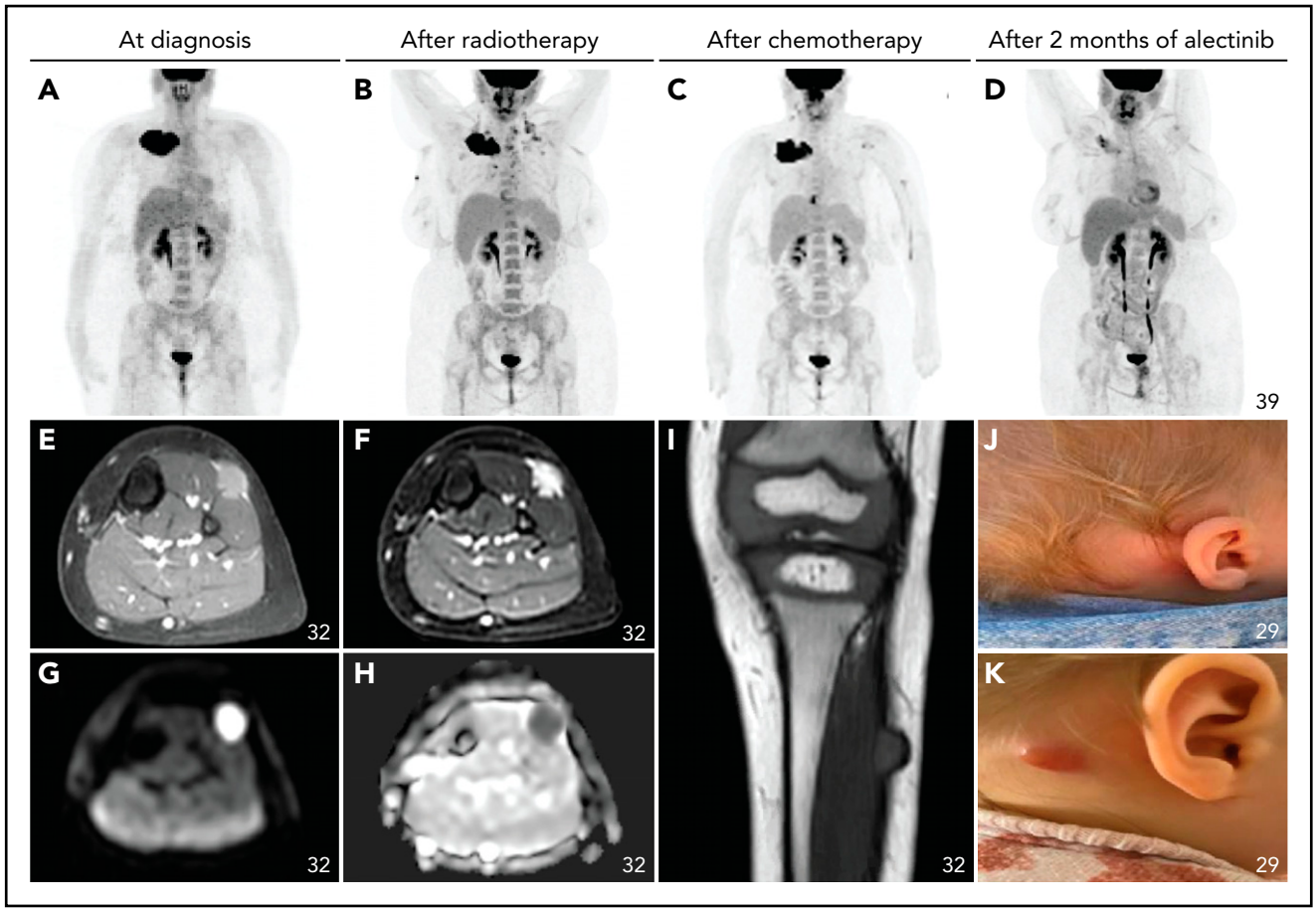

Figure 5. Nonneurologic disease manifestations in ALK-positive histiocytosis patients with single-system disease (Group 2). (A-D) Successive fluorodeoxyglucose PET-CT images of an adult female with a large right clavicular tumor at diagnosis (A; time, 0) and after treatment with radiotherapy (B; time, 5.5 months), 6 weeks of vinblastine/prednisone-based chemotherapy (C; time, 9.5 months), and 2 months of alectinib (D; time, 14 months). (E-I) T1-weighted contrast-enhanced (E), T2-weighted (F), diffusion-weighted (G), apparent diffusion coefficient (H), and plain T1-weighted (I) MRI images of the left lower leg of a child at diagnosis showing a single soft tissue tumor that infiltrates the musculature and shows contrast enhancement and restricted diffusion. (J-K) Photographs of the retroauricular scalp lesion of an infant, with a clear change in clinical appearance after 3 months (K).

Responses to ALK inhibition were durable in 7/7 patients, with no events of progression or relapse on treatment (Figure 7).

Group 2 First-line treatment consisted of surgical resection in 13/23, radiation in 1/23, conventional systemic therapy with or without local therapy in 4/23, and ALK inhibition in 1/23 patients (Table 2). Furthermore, 1/23 patients was observed without treatment, 1/23 was not treated yet, and 2/23 were lost to follow-up. Of those with local therapy, 2/14 had progressive disease. Of patients treated with conventional systemic therapy, 3/4 had an objective response, and 1/4 had progressive disease. The patient treated with ALK inhibition had an objective response. Second-line treatment was given to 4 patients. ALK inhibition was administered in 2/4 patients with objective response, whereas the 2 others received chemotherapy with progressive disease. Third-line treatment with ALK inhibition was initiated in 1 of these patients with objective response (Figure 5A-D). Responses to ALK inhibition were durable in 4/4 patients (Figure 7).

Histopathologic features

The morphology of ALK-positive histiocytoses varied and included classic xanthogranuloma features with plump foamy histiocytes and variable Touton giant cells in 12/39 (31%) patients (Figure 8A-B) to a more densely cellular, monomorphic appearance without lipidized histiocytes in the majority of cases (Figure 8C,E), some with more spindled/streaming or epithelioid histiocyte morphology (supplemental Table 1). Nuclear features included ovoid nuclei that frequently displayed either a slight fold or indentation (ie, "cup shape") of its nuclear contour. Mild atypia was limited to 6/39 cases, often with an epithelioid phenotype, which can be confused with malignant

Figure 4 (continued) nerves, highly reminiscent of nerve sheath tumors such as neurofibromas. (J-N) Axial images of successive T1-weighted contrast-enhanced MRI scans of the head of a child with a left insula tumor before and after subtotal resection and successful treatment with alectinib. (O-Q) Axial images of the T1-weighted contrast-enhanced MRI scans of the head of a child with a left oculomotor nerve tumor, demonstrating slight regression but continued contrast enhancement of the tumor after treatment with vinblastine/prednisone-based chemotherapy. (R) Coronal image of the T1-weighted contrast-enhanced MRI scan of the head showing a 30 × 25 × 34 mm large tumor with contrast enhancement in the prepontine cistern that followed the course of the trigeminal nerve and caused pressure on the pons. (S) Sagittal image of the T1-weighted contrast-enhanced MRI scan of the cervical spine showing a large (18 × 24 × 45 mm) intradural extramedullary tumor at level C1-C2.

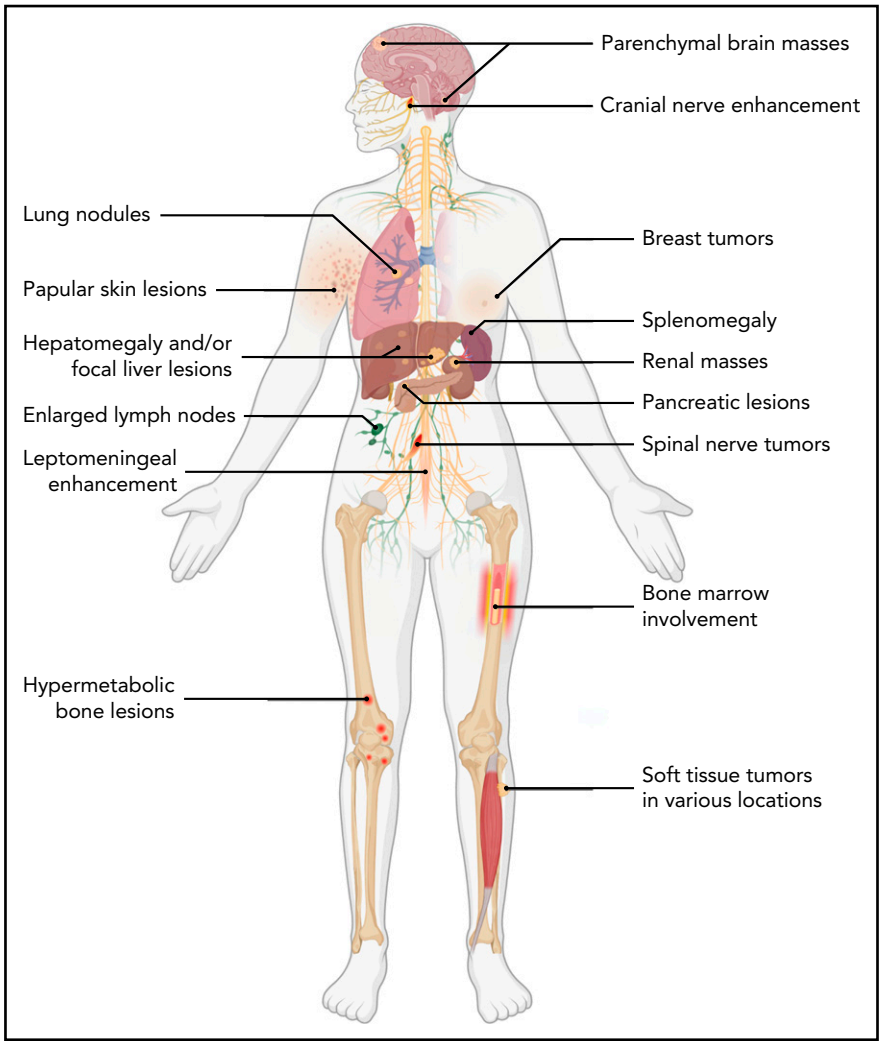

Figure 6. Body diagram showing recurrent anatomic sites of involvement of ALK-positive histiocytosis.

histiocytosis; however, mitotic counts and Ki-67 proliferation indexes were low to moderate. Bone marrow involvement was typically a small amount and not a diffuse infiltrative process as in leukemia. The morphology was that of plump histiocytes with indented nuclei and a juvenile xanthogranuloma (JXG)-like phenotype in normo- to hypercellular bone marrow with relatively preserved hematopoiesis and occasional eosinophilia, mild myelofibrosis, and/or megakaryocytic hyperplasia.

The ALK staining pattern did not appear to correlate with molecular alteration as the frequent *KIF5B-ALK* fusion was noted with all stain patterns; however, no (convincing) nuclear ALK staining was observed. Four cases displayed focal weak ALK staining and 3/39 had exclusive cytoplasmic Golgi dot-like staining in the lesional histiocytes (Figure 8I; Table 4) despite confirmed *ALK* fusions. Almost half of cases had variable Rosai-Dorfman disease–like histologic features including S100 expression (18/39) and emperipolesis (13/39). When tested for OCT-2 expression,[58] 14/23 (61%) were positive. When tested for *p*-ERK (18/39) and Cyclin D1 (19/39) expression (supplemental Table 1), the lesional histiocytic cells often showed corresponding, strong expression (Figure 8K-L).

Molecular pathologic features

ALK rearrangements were confirmed in 37/39 patients (Table 1). In 2 infants from Group 1A with classic systemic disease, similar to the cases described by Chan et al,[29] no *ALK* rearrangements were detected by FISH; however, the material was insufficient for comprehensive analysis by RNA-seq. *KIF5B* was the most common *ALK* fusion partner and identified in 27 cases, with exon 24 of *KIF5B* fused to exon 20 of *ALK* in 25/27 cases (supplemental Table 3). In addition, *CLTC-ALK, TPM3-ALK, TFG-ALK, EML4-ALK,* and *DCTN1-ALK* fusions were detected in single cases (supplemental Figure 1).

Atypical *ALK*-rearranged histiocyte-rich tumors: a potential diagnostic pitfall

Three cases were identified without macrophage/histiocyte marker expression by the ALK$^+$ tumor cells but with prominent intermixed CD163-expressing (reactive) macrophages (supplemental Figure 2), which can be mistaken for ALK-positive histiocytosis. Moreover, by hematoxylin and eosin stain, the tumor cells often had similar morphology as those seen in ALK-positive histiocytosis, consisting of plump mononucleated

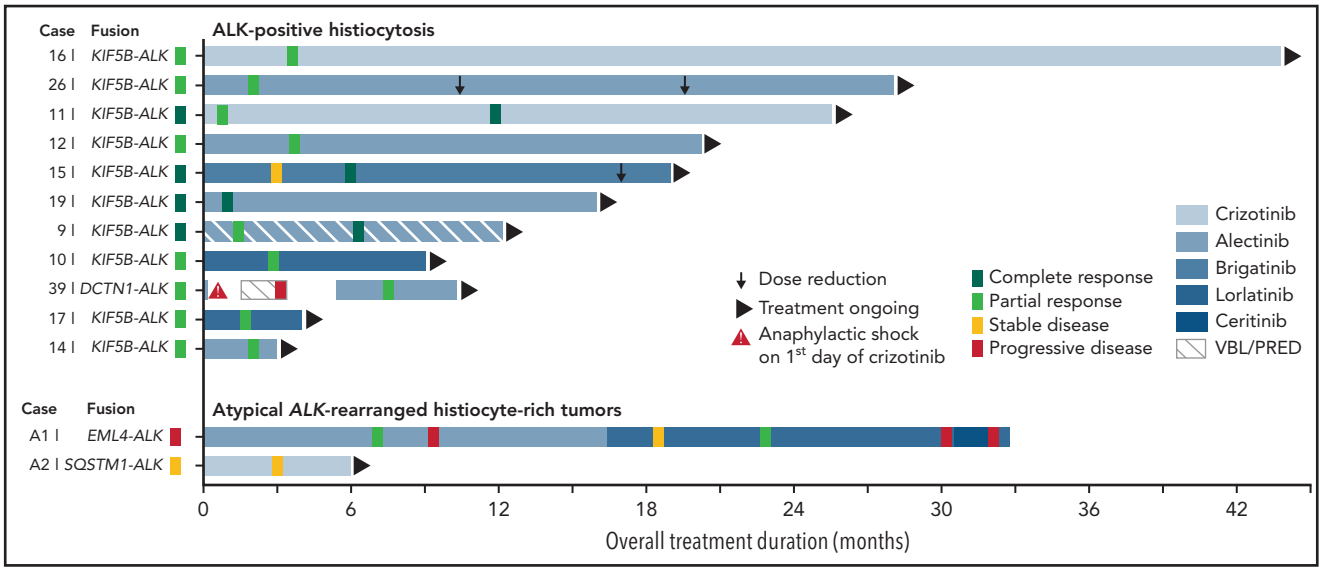

Figure 7. Swimmer plot of outcomes in patients with ALK-positive histiocytosis (n = 11) or atypical *ALK*-rearranged histiocyte-rich tumors (n = 2) treated with ALK inhibition. ALK inhibition was initiated at timepoint zero. Median time on ALK inhibition was 16 months in ALK-positive histiocytosis patients (range 3-43 months). Responses were measured by CT, MRI, and/or PET-CT in all patients. Dose reductions were 67% (90 mg brigatinib/d → 30 mg/d) and 50% (1200 mg alectinib/d → 900 mg/d → 600 mg/d) in Case 15 and Case 26, respectively. Case 39 developed a severe (grade 3) anaphylactic shock on the first day of crizotinib administration, requiring the patient to be resuscitated. The patient subsequently received vinblastine/prednisone-based chemotherapy with progressive disease and then switched to alectinib with objective response after 2 months. Case A1 developed a subcutaneous gluteal metastasis during treatment with alectinib (supplemental Figure 3C), which was found to harbor an *ALK* p.I1171N mutation, a mutation known to confer secondary resistance to alectinib.[78,79] Therefore, the patient switched to lorlatinib and later to ceritinib after repeated progressive disease. Due to continuing progressive disease during treatment with ceritinib, the patient recently stopped ceritinib, received 3 weeks of bridging therapy with lorlatinib during antalgic radiotherapy of 2 metastases, and subsequently started vinblastine/prednisone-based chemotherapy. VBL/PRED, vinblastine and prednisone-based chemotherapy.

cells with eosinophilic cytoplasm. In addition, the lesional cells demonstrated *p*-ERK and/or Cyclin D1 expression (supplemental Figure 2). Despite extensive immunohistochemical and molecular pathologic analysis, no definitive diagnosis could be made for the 3 cases. The ALK$^+$ cells lacked immunoreactivity for many lineage markers, including CD30 and smooth muscle actin (supplemental Table 1). Moreover, clonality assessment of T-cell receptor and Ig gene rearrangements did not reveal high monoclonal peaks (supplemental Methods), arguing against a type of lymphoma. CD34 immunostains did reveal a remarkable nested, endocrinoid to hemangiopericytoma-like pattern with abundant blood capillaries in all 3 cases (supplemental Figure 2). None had the *KIF5B-ALK* fusion but rather harbored *ALK* fusions involving *EML4* or *SQSTM1*.

Clinically, 1 of the 3 patients was an adult with Group 1B–like multisystemic disease involving the CNS, left lung, and bone (Case A1; supplemental Figure 3A-D). This patient initially had an objective response to ALK inhibition but then demonstrated disease progression and switched to chemotherapy (Figure 7; Table 3). The remaining 2 cases had Group 2–like single-system disease with localized soft tissue tumors. Both were treated with surgery; however, 1 relapsed with subcutaneous and liver metastases (Case A2; supplemental Figure 3E-F) and received systemic treatment with ALK inhibition with stable disease after 3 months of crizotinib.

ALK-immunoreactive histiocytoses without *ALK* rearrangements

Ten patients were identified with histiocytoses demonstrating variable ALK immunoreactivity (supplemental Figure 4) but no *ALK* rearrangement by RNA-seq. Both clinically and histologically, these cases represented the full spectrum of histiocytic neoplasms, from L-, C-, and *R*- to M-group (supplemental Table 4).[1] When compared with ALK-positive histiocytoses, they more often showed nuclear ALK staining. Other MAPK activating somatic mutations were identified in 5/10 patients.

Discussion

We present here a collaborative international study of ALK-positive histiocytosis with detailed clinicopathologic data of 39 cases, including 37 cases with confirmed *ALK* rearrangements. This study defines a new clinicopathologic spectrum and highlights frequent neurologic involvement. Histology included classic xanthogranuloma features in almost one-third of patients, whereas the majority displayed a more densely cellular, monomorphic appearance without lipidized histiocytes. We affirm the frequent occurrence of *KIF5B-ALK* fusions[43] and expand the molecular spectrum by describing single cases with *CLTC-ALK*, *TPM3-ALK*, *TFG-ALK*, *EML4-ALK*, or *DCTN1-ALK* fusions. Finally, we show dramatic and durable responses in 11/11 patients treated with ALK inhibition (Figure 7), 10 with neurologic involvement.

We noted an apparent predilection for females in our cohort of ALK-positive histiocytosis cases, consistent with our overview of the existing literature (supplemental Table 5) and the female predilection observed in *ALK*-rearranged tumors other than non–small cell lung cancer,[50] such as *ALK*-rearranged inflammatory myofibroblastic tumors.[59] This female

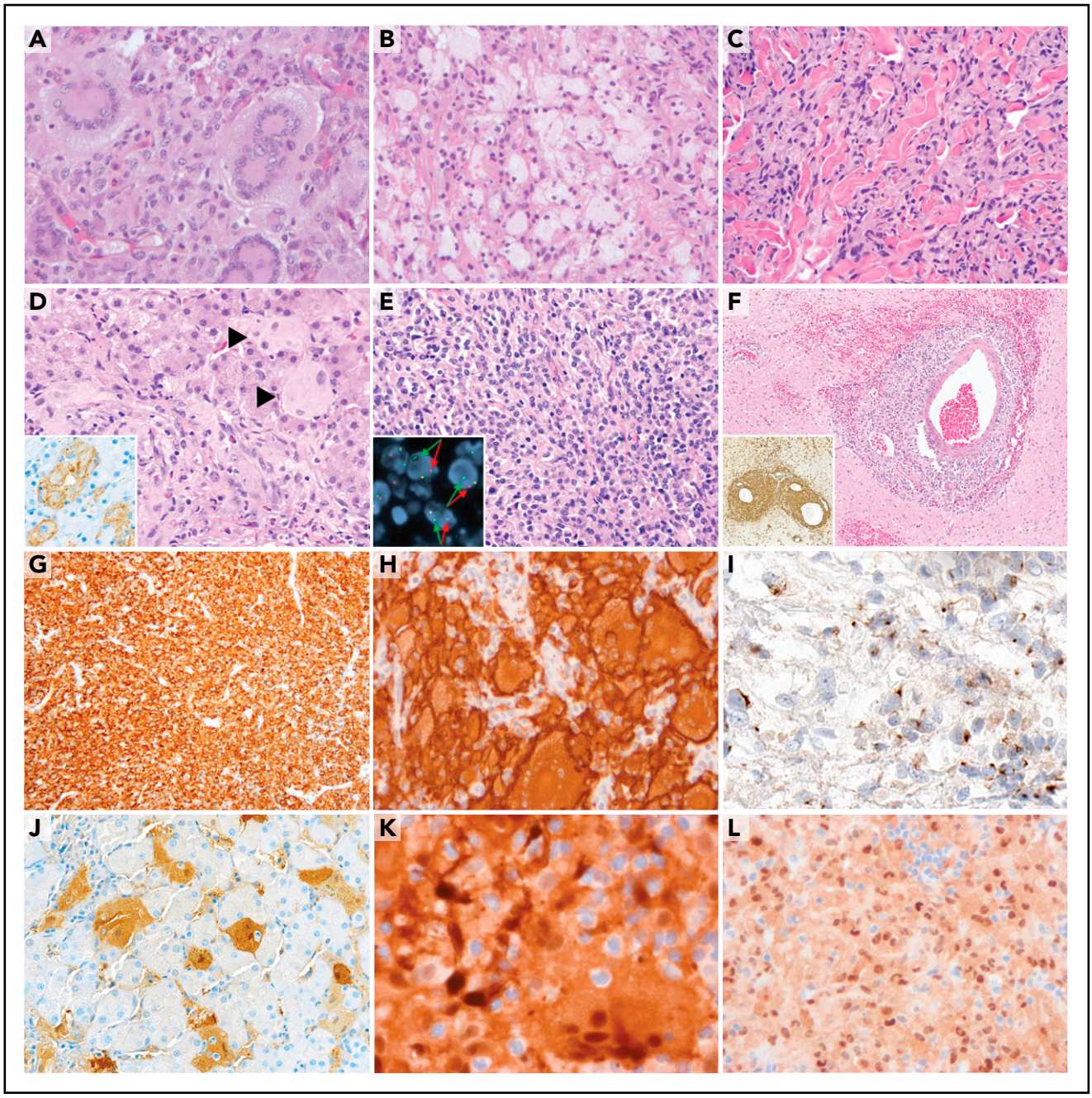

Figure 8. Histopathologic features of ALK-positive histiocytosis. (A) Photomicrograph of the hematoxylin and eosin (HE)-stained slide of a frontal bone tumor (Case 7; original magnification ×200) with classic xanthogranuloma morphology including many Touton giant cells. (B) HE image of a spinal nerve root tumor (Case 15; original magnification ×200) showing abundant lipidized ("foamy") histiocytes. (C) HE image (Case 31; original magnification ×400) showing a more monomorphic histiocytic infiltrate in the skin dissecting through the dermal collagen bundles. (D) HE image of a liver biopsy (Case 4; original magnification ×400) showing sinusoidal infiltration by large histiocytes (indicated by black arrows) with ALK immunoreactivity (inlet). (E) HE image of a CNS tumor (Case 18; original magnification ×400) with a monomorphic, dense infiltrate of histiocytes that demonstrate separated red and green signals on *ALK* break-apart FISH analysis (inlet). (F) HE image of a CNS lesion (Case 20; ×100) showing marked infiltration of the perivascular ("Virchow-Robin") spaces by histiocytes with clear CD163 immunoreactivity (inlet). (G) CD163 immunostain of a CNS tumor (Case 18; original magnification ×200) showing diffuse strong expression by the monomorphic histiocytic infiltrate. (H) ALK immunostain (Case 7; original magnification ×200) showing strong cytoplasmic and membranous staining of lesional histiocytes and Touton giant cells. (I) ALK immunostain of a breast tumor (Case 12; original magnification ×400) showing focal, exclusive dot-like immunoreactivity that could be misinterpreted as negative. (J) S100 immunostain of a liver biopsy (Case 4; ×200) showing immunoreactivity by the large sinusoidal histiocytes. (K) P-ERK immunostain (Case 15; original magnification ×400) showing diffuse positive staining by the lesional cells, as well as clear emperipolesis (intact intracytoplasmic leukocytes). (L) Cyclin D1 immunostain of an oculomotor nerve tumor (Case 21; original magnification ×200) showing cytoplasmic and strong nuclear staining in histiocytes with frequent nuclear indentations.

predilection is in clear contrast to the male predominance in LCH,[60,61] ECD,[62,63] and JXG,[64,65] particularly in *BRAF* p.V600E–associated CNS lesions with JXG histology.[28]

Our Group 1A patients were similar to the cases originally described by Chan et al.[29] In addition to liver, spleen, and hematopoietic involvement, our patients had lesions in the

Table 4. Histopathologic and molecular characteristics of ALK-positive histiocytoses

No.	*ALK* rearrangement	Analysis method(s)	Classic XG-like	Emperipolesis	ALK IHC	
					Staining	Staining pattern
Group 1A						
1	Not confirmed	*ALK*-FISH negative; *KIF5B-ALK* RT-PCR negative; no RNA-seq (insufficient material)	No	Yes	Positive	Light cytoplasmic; membranous
2	*ALK*-FISH+	FISH	No	Yes abundant	Positive	Diffuse cytoplasmic; membranous
3	*KIF5B-ALK*	Archer FusionPlex targeted RNA-seq	No	No	Positive	Granular cytoplasmic with focal Golgi dot-like accentuation; no membranous
4	Not confirmed	*ALK*-FISH negative; no RNA-seq (insufficient material)	Yes	Yes abundant	Positive	Scant cytoplasmic; strong membranous
5	*ALK*-FISH+	FISH	Yes	Yes	Positive	Weak cytoplasmic; strong membranous
6	*CLTC-ALK*	Archer FusionPlex targeted RNA-seq	No	Yes	Positive	Diffuse dark cytoplasmic (clone 5A4) to more light granular cytoplasmic (clone ALK1); membranous (both)
Group 1B						
7	*TPM3-ALK*	Archer FusionPlex targeted RNA-seq	Yes	Yes	Positive	Diffuse cytoplasmic with Golgi dot-like accentuation; membranous
8	*ALK*-FISH+	FISH	No	No	Positive	Diffuse granular cytoplasmic with rare Golgi dot-like accentuation; no membranous
9	*KIF5B-ALK*	Illumina Childhood Cancer targeted RNA-seq	No	No	Weak	Very weak diffuse cytoplasmic; no membranous
10	*KIF5B-ALK*	Illumina Trusight targeted RNA-seq	No	No	Positive	Diffuse dark cytoplasmic (clone D5F3) to more light, granular cytoplasmic with Golgi dot-like accentuation (clone ALK1); no membranous
11	*KIF5B-ALK*	Archer FusionPlex targeted RNA-seq	No	No	Positive	Diffuse cytoplasmic; no membranous
12	*KIF5B-ALK*	*KIF5B-ALK* RT-PCT positive	No	No	Exclusive dot-like	Golgi dot-like cytoplasmic only; no membranous
13	*TFG-ALK*	Archer FusionPlex targeted RNA-seq	Yes	No	Focal, weak	Very weak cytoplasmic blush to negative; no membranous
14	*KIF5B-ALK*	Archer FusionPlex targeted RNA-seq	No	No	Positive	Granular cytoplasmic with Golgi dot-like accentuation; no membranous
15	*KIF5B-ALK*	Archer FusionPlex targeted RNA-seq	Yes	Yes	Positive	Diffuse cytoplasmic with Golgi dot-like accentuation; no membranous
16	*KIF5B-ALK*	Archer FusionPlex targeted RNA-seq	No	No	Positive	Granular cytoplasmic with rare Golgi dot-like accentuation; no membranous

RT-PCR, reverse transcription polymerase chain reaction; XG, xanthogranuloma.

*Multiple areas with xanthomatous histiocytes and Touton giant cells were observed; however, a significant part consisted of an infiltration of spindly cells.

Table 4. (continued)

No.	*ALK* rearrangement	Analysis method(s)	Classic XG-like	Emperipolesis	ALK IHC	
					Staining	Staining pattern
Group 2: neurological involvement						
17	*KIF5B-ALK*	FoundationOne Heme targeted RNA-seq	No	No	Positive	Granular cytoplasmic with Golgi dot-like accentuation in some cells; no membranous
18	*ALK*-FISH+	FISH	No	No	Positive	Diffuse cytoplasmic with Golgi dot-like accentuation; membranous
19	*KIF5B-ALK*	Archer FusionPlex targeted RNA-seq	No	No	Positive	Diffuse cytoplasmic; no membranous
20	*KIF5B-ALK*	FoundationOne Heme targeted RNA-seq	No	No	Focal, weak	Focal, weak diffuse cytoplasmic with Golgi dot-like accentuation; no membranous
21	*KIF5B-ALK*	Archer FusionPlex targeted RNA-seq	Yes	Yes	Positive	Diffuse cytoplasmic with Golgi dot-like accentuation; no membranous
22	*KIF5B-ALK*	Whole transcriptome RNA-seq	No	No	Positive	Diffuse granular cytoplasmic; no membranous
23	*KIF5B-ALK*	Whole transcriptome RNA-seq	No	No	Positive	Diffuse granular cytoplasmic; no membranous
24	*ALK*-FISH+	FISH	Yes*	No	Positive	Diffuse granular cytoplasmic; no membranous
25	*KIF5B-ALK*	Archer FusionPlex targeted RNA-seq	Yes	Yes abundant	Positive	Diffuse cytoplasmic with Golgi dot-like accentuation; membranous
26	*KIF5B-ALK*	Ion Ampliseq RNA Fusion Lung Cancer targeted RNA-seq; whole transcriptome RNA-seq	No	Yes abundant	Positive	Diffuse cytoplasmic with Golgi dot-like accentuation; no membranous
27	*KIF5B-ALK*	Archer FusionPlex targeted RNA-seq	Yes	No	Positive	Diffuse granular cytoplasmic; no membranous
28	*KIF5B-ALK*	FoundationOne Heme targeted RNA-seq	No	No	Focal, weak	Variable focal, weak cytoplasmic to negative; no membranous
Group 2: nonneurological involvement						
29	*KIF5B-ALK*	Archer FusionPlex targeted RNA-seq	No	No	Positive	Diffuse cytoplasmic with Golgi dot-like accentuation; no membranous
30	*KIF5B-ALK*	Oncomine Comprehensive Assay Plus targeted RNA-seq	No	No	Positive	Diffuse granular cytoplasmic with Golgi dot-like accentuation; no membranous
31	*KIF5B-ALK*	Archer FusionPlex targeted RNA-seq	No	No	Positive	Diffuse granular cytoplasmic; no membranous
32	*KIF5B-ALK*	Whole transcriptome RNA-seq	No	No	Positive	Diffuse dark cytoplasmic; subset possibly nuclear; no membranous (clone 5A4, lung staining protocol). Focal/ Golgi dot-like cytoplasmic; no nuclear or membranous (clone 5A4, lymphoma staining protocol)

RT-PCR, reverse transcription polymerase chain reaction; XG, xanthogranuloma.

*Multiple areas with xanthomatous histiocytes and Touton giant cells were observed; however, a significant part consisted of an infiltration of spindly cells.

Table 4. (continued)

No.	*ALK* rearrangement	Analysis method(s)	Classic XG-like	Emperipolesis	ALK IHC	
					Staining	Staining pattern
33	*KIF5B-ALK*	Illumina Trusight targeted RNA-seq	No	Yes	Positive	Diffuse light granular cytoplasmic with dark Golgi-dot like accentuation; no membranous
34	*KIF5B-ALK*	Illumina Trusight targeted RNA-seq	No	No	Exclusive dot-like	Golgi dot-like cytoplasmic only (focal weak); no membranous
35	*KIF5B-ALK*	Archer FusionPlex targeted RNA-seq	No	No	Positive	Diffuse granular cytoplasmic with Golgi dot-like accentuation; no membranous
36	*KIF5B-ALK*	FoundationOne Heme targeted RNA-seq	No	No	Exclusive dot-like	Golgi dot-like cytoplasmic only (focal weak); no membranous
37	*KIF5B-ALK*	Archer FusionPlex targeted RNA-seq	Yes	Yes	Positive	Diffuse cytoplasmic with Golgi dot-like accentuation; membranous
38	*EML4-ALK*	Archer FusionPlex targeted RNA-seq	Yes	No	Positive	Diffuse granular cytoplasmic; membranous
39	*DCTN1-ALK*	Archer FusionPlex targeted RNA-seq	Yes	Yes abundant	Positive	Diffuse cytoplasmic with Golgi dot-like accentuation; membranous

RT-PCR, reverse transcription polymerase chain reaction; XG, xanthogranuloma.

*Multiple areas with xanthomatous histiocytes and Touton giant cells were observed; however, a significant part consisted of an infiltration of spindly cells.

lungs, kidneys, and/or skin. Unlike in LCH,[66] in which liver, spleen, and/or hematopoietic involvement constitutes "risk organ" involvement associated with increased mortality, this clinical phenotype in ALK-positive histiocytosis does not necessarily comprise high-risk disease as 2 of 6 patients from Group 1A had spontaneous regression of disease with only supportive care. However, of the 3 other patients with clinical follow-up, 3/3 required second-line systemic therapy and 1 died, underscoring the life-threatening condition that this disease can still represent.[29]

Other patients with multisystemic ALK-positive histiocytosis (Group 1B) have been variably reported previously (supplemental Table 5), sometimes as ECD or systemic JXG. The nervous system was the most frequently involved organ in our patients from this group, followed by the lungs, bone, liver, skin, and lymph nodes. Although there are similarities between patients from this group and patients with ECD, particularly bilateral bone lesions in the legs, many other stigmata of ECD were not observed. For example, perinephric soft tissue thickening ("hairy kidneys"), periaortic encasement, diabetes insipidus, and right atrial infiltration are frequent in ECD[62,67] but were absent in our cohort. Moreover, ECD patients are generally older, with a median age of 55 years,[2,63] as opposed to a median age of 14.5 years of our Group 1B patients. Apart from the specific phenotypic entity that is ECD, there exists the constellation of "extracutaneous/systemic JXG,"[68,69] referring to the rare disease in childhood with JXG histology involving extracutaneous tissues. In a recent series of "systemic JXG," associations were observed between specific molecular alterations and clinical phenotypes, with *ALK* rearrangements overrepresented in female cases and cases with lung involvement.[68] These findings are compatible with ours, raising the question whether ALK-positive histiocytosis is distinct from "systemic JXG" without *ALK* rearrangements. Altogether, although there is overlap in histomorphology and immunophenotype, we believe that sufficient evidence is available for the designation of ALK-positive histiocytosis as a separate histiocytic entity from both ECD and "extracutaneous/systemic JXG" as previously proposed by others.[45]

The findings in our patients with single-system disease (Group 2) were similar to that which has been observed previously (supplemental Table 5), with the nervous system and skin/soft tissue as common sites of disease and surgical resection often being definitive. We expand the clinical spectrum by describing patients with localized bone involvement. When compared with previously reported cases with single-system disease, our cohort includes more cases with isolated neurologic involvement (52% vs 19%) and more children (87% vs 38%). Given the retrospective nature of our study, we cannot rule out some selection bias influencing the clinical spectrum of the disease in our cohort. For example, our cohort did not include adult female patients with isolated breast masses as recently described by Kashima et al[34] and Osako et al.[41] Yet, our study did include 2 patients with multisystemic disease including breast masses (Table 3; Figure 3R), supporting the recurrent involvement of this anatomic site.

Eleven patients in our cohort were treated with diverse ALK inhibitors, either as first- or second- or further-line therapy, and sustained objective responses were observed in 11/11 patients (Figure 7). These data corroborate the favorable outcomes of ALK inhibition observed in 7 ALK-positive histiocytosis patients outside of our cohort.[33,34,40,43,50,51] Our patients were treated with various ALK inhibitors at variable doses; however, the impression of their efficacy is unequivocal. The responses to ALK inhibition stand in contrast to outcomes with conventional systemic therapy, which conferred an objective response in only 7/13 (54%) patients as first-line therapy and 2/5 (40%) patients as second-line therapy (Table 2). However, given that this is a retrospective study, it remains undefined whether ALK inhibition should be implemented as first-line treatment or when disease is refractory to conventional therapies. Also, our study does not address the optimal treatment regimen or duration for ALK inhibition, which is an enduring question for targeted therapy of histiocytosis more broadly, as cessation of BRAF inhibition in histiocytosis patients has been shown to lead to early relapses in most cases.[22,26,70]

As illustrated by the 3 "atypical *ALK*-rearranged histiocyte-rich tumors," stringent histopathologic assessment is essential before making a diagnosis of ALK-positive histiocytosis. Diagnosis requires diffuse expression of macrophage/histiocyte markers, preferably CD163, by the lesional ALK$^+$ tumor cells. *ALK*-rearranged tumors with prominent intermixed histiocytic infiltrates disparate from ALK$^+$ cells without immunoreactivity for macrophage/histiocyte markers are a potential diagnostic pitfall and should be assessed for the possibility of representing another *ALK*-rearranged entity, such as inflammatory myofibroblastic tumors, which typically do not harbor *KIF5B-ALK* fusions.[71,72] Future studies may elucidate whether "atypical *ALK*-rearranged histiocyte-rich tumors" without characteristics of established (*ALK*-rearranged) entities comprise a new entity. In all 3 of our cases, the CD34 immunostain revealed a remarkable nested pattern with abundant blood capillaries (supplemental Figure 2), which was also observed in a case previously reported as ALK$^+$histiocytosis with unusual morphology and a *TRIM33-ALK* fusion.[32] Clinically, this patient had a large mesenteric tumor, highly similar to Case A2 from our study (supplemental Figure 3E-F). Finally, the monomorphic dense infiltration of histiocytes seen in the majority of our ALK-positive histiocytosis cases should be distinguished from epithelioid fibrous histiocytoma.[73]

Supported by our 10 excluded histiocytosis cases demonstrating variable ALK immunoreactivity but no *ALK* rearrangement by RNA-seq, molecular confirmation of *ALK* rearrangement should be performed whenever possible to confirm the diagnosis of ALK-positive histiocytosis. This is important because cases with ALK staining but without *ALK* rearrangements may not benefit from ALK inhibition.[74,75] ALK IHC should particularly be applied in the diagnostic workup of infants with classic multisystemic disease and patients with tumorous lesions in the nervous system, lungs, bone, and/or soft tissue with non-LCH histology. Yet, pathologists should be aware of the variable staining intensity and pattern, with variations further compounded by the ALK clone and protocol used. Comprehensive molecular analysis (ie, RNA-seq) should be performed in ALK IHC–negative cases when the detection of an *ALK* rearrangement could have treatment consequences as we noted in 7 confirmed *ALK*-rearranged cases weak or exclusive Golgi dot-like cytoplasmic ALK staining that could be misinterpreted as negative.

Overall, this study defines a new clinicopathologic spectrum of ALK-positive histiocytosis with frequent neurologic involvement and durable responses to ALK inhibition. The findings support

the recognition of ALK-positive histiocytosis as a distinct entity from both ECD and (extracutaneous/systemic) JXG. Comprehensive genomic analysis of patients with histiocytic neoplasms is now a necessary adjunct to detailed morphologic and immunophenotypic assessment as this may directly affect disease classification and therapeutic decision making.

Acknowledgments

The authors acknowledge the International Rare Histiocytic Disorders Registry (IRHDR, ClinicalTrial.gov number NCT02285582), which included some patients described in this study. The authors thank Chris Woods (Lead Analyst, Imaging Informatics) and the Research Pathology Laboratory at Cincinnati Children's Hospital Medical Center, John DeCoteau (molecular pathologist) at University of Saskatchewan, Sven van Kempen (senior laboratory technician) and Lennart Kester (clinical molecular biologist in pathology in training) at Princess Máxima Center for Pediatric Oncology, and Demi van Egmond (laboratory technician), Tom van Wezel (clinical molecular biologist in pathology), and Arjen Cleven (pathologist) at Leiden University Medical Center for technical assistance. The authors thank Els Wauters (pulmonologist and respiratory oncologist) at University Hospitals Leuven, Andreas Rosenwald (pathologist) at the Institute of Pathology of the University of Würzburg, and Bipin Mathew (pathologist) at Leeds Teaching Hospitals for clinical care and/or diagnostics of patients described in this study. The authors thank Les Laboratoires Servier for allowing the use of their medical illustrations (Servier Medical Art, https://smart.servier.com) in the visual abstract. Figure 6 was created with BioRender.com.

P.G.K. received a grant from Leiden University Medical Center. A.G.S.v.H. is supported by Stichting 1000 kaarsjes voor Juultje. E.L.D. is supported by the National Institutes of Health/National Cancer Institute Core Grant (P30 CA008748), National Cancer Institute (R37 CA259260-01), the Frame Fund, Applebaum Foundation, and Joy Family West Foundation. J.-F.E. is supported by the Programme de Recherche Translationnelle sur le Cancer from the French National Cancer Institute (PRT-K19-143).

Authorship

Contribution: P.G.K., J.P., E.L.D., and J.-F.E. conceived the study and drafted the manuscript; J.P. and J.-F.E. performed the central pathology review and provided histologic images; P.G.K., J.P., B.H.D., Z.H.-R., L.H.-J., and J.-F.E. performed additional immunohistochemical and/or molecular analyses; P.G.K. made the figures; A.G.S.v.H. participated in data discussions; A.G.S.v.H. and O.A. provided supervision; and all authors contributed cases, and read, revised, and approved the manuscript (meeting the International Committee of Medical Journal Editors criteria for authorship).

Conflict-of-interest disclosure: E.L.D. discloses unpaid editorial support from Pfizer Inc and paid advisory board membership from Day One Biopharmaceuticals outside the submitted work. M.E. discloses honoraries and travel grants by Jazz Pharmaceuticals, Merck Sharp & Dohme, and Amgen. V.P. discloses giving lectures supported by Sanofi, R-farma, and Roche and participation in an expert board supported by Novartis. J.L.H. is a consultant to Aadi Biosciences and TRACON Pharmaceuticals outside the scope of the manuscript. The remaining authors declare no competing financial interests.

ORCID profiles: P.G.K., 0000-0001-9793-7032; J.P., 0000-0002-3718-6422; B.H.D., 0000-0001-8090-5448; Z.H.-R., 0000-0001-9341-7494; L.H-J., 0000-0002-0332-1673; C.v.d.B., 0000-0002-6175-6077; C.J.M.v.N., 0000-0001-7907-7390; J.A.M.v.L., 0000-0002-8885-4929; R.M.V., 0000-0003-1437-214X; U.E.F., 0000-0003-0315-4307; P.C.W.H., 0000-0002-1513-8104; F.J.S.H.W.-A-J., 0000-0001-7840-6156; R.S., 0000-0003-2244-5839; A.B., 0000-0002-7905-7696; F.F., 0000-0002-1234-982X; M.E., 0000-0002-4229-8058; F.F., 0000-0002-5496-293X; V.W., 0000-0002-2802-4034; O.G-K., 0000-0003-3376-5432; B.D-B., 0000-0002-3845-5380; D.A.E., 0000-0001-8610-0624; V.P., 0000-0003-2985-0503; V.V.B., 0000-0002-9191-5091; S.G., 0000-0002-1387-0836; S.R., 0000-0002-1477-8855; M.G., 0000-0002-0461-1445; G.T., 0000-0002-7139-5711; S.H., 0000-0003-0384-6370; J.D., 0000-0002-4485-146X; L.F., 0000-0002-2612-7574; S.F., 0000-0002-2258-2051; M-L.J., 0000-0002-0048-6501; M.C., 0000-0001-6585-9586; K.T., 0000-0003-2528-6992; P.M.B., 0000-0002-2628-9653; I.S.T., 0000-0002-1435-944X; D.E.D., 0000-0003-1939-7338; B.E., 0000-0002-1917-1630; A.R., 0000-0001-6198-7441; M.S., 0000-0002-9858-4707; J.L.W., 0000-0003-0585-9669; I.E., 0000-0001-9930-7990; B.A.S., 0000-0002-2456-2476; L.R.M., 0000-0002-0479-5950; J.L.H., 0000-0001-6475-8345; S.A., 0000-0001-9246-4184; K.K.Y., 0000-0003-0713-6384; K.P-D., 0000-0002-4048-8376; S.Z.P., 0000-0001-5964-5565; L.S.M-A., 0000-0002-0229-9056; D.G.L., 0000-0001-9183-5617; D.D.G., 0000-0003-1899-4755; S.R., 0000-0002-5681-0112; A.R.K., 0000-0002-8306-8419; M.M.H., 0000-0002-3624-0706; A.G.S.v.H., 0000-0002-0563-4155; O.A., 0000-0001-7446-6274; E.L.D., 0000-0001-5456-5961; J-F.E., 0000-0002-6073-4466.

Correspondence: Jennifer Picarsic, Division of Pathology, Cincinnati Children's Hospital Medical Center, 3333 Burnet Ave, ML 1035, Cincinnati, OH 45229; e-mail: jennifer.picarsic@cchmc.org; Eli L. Diamond, Department of Neurology, Memorial Sloan-Kettering Cancer Center, 160 East 53rd St, 2nd Floor Neurology, New York, NY 10022; e-mail: diamone1@mskcc.org; and Jean-François Emile, EA4340 Laboratory and Department of Pathology, Ambroise Paré Hospital, 9 Avenue Charles de Gaulle, 92104 Boulogne, France; e-mail: jean-francois.emile@uvsq.fr.

Footnotes

Submitted 19 July 2021; accepted 18 October 2021; prepublished online on *Blood* First Edition 2 November 2021. DOI 10.1182/blood.2021013338.

*P.G.K. and J.P. are joint first authors and contributed equally to this study.

†E.L.D. and J.-F.E. are joint last authors and contributed equally to this study.

Original data are available from the corresponding authors upon reasonable request.

There is a *Blood* Commentary on this article in this issue.

The online version of this article contains a data supplement.

REFERENCES

1. Emile J-F, Abla O, Fraitag S, et al; Histiocyte Society. Revised classification of histiocytoses and neoplasms of the macrophage-dendritic cell lineages. *Blood*. 2016;127(22):2672-2681.
2. Emile J-F, Cohen-Aubart F, Collin M, et al. Histiocytosis. *Lancet*. 2021;398(10295):157-170.
3. Badalian-Very G, Vergilio J-A, Degar BA, et al. Recurrent BRAF mutations in Langerhans cell histiocytosis. *Blood*. 2010;116(11):1919-1923.
4. Haroche J, Charlotte F, Arnaud L, et al. High prevalence of BRAF V600E mutations in Erdheim-Chester disease but not in other non-Langerhans cell histiocytoses. *Blood*. 2012;120(13):2700-2703.
5. Lee LH, Gasilina A, Roychoudhury J, et al. Real-time genomic profiling of histiocytoses identifies early-kinase domain BRAF alterations while improving treatment outcomes. *JCI Insight*. 2017;2(3):e89473.
6. Durham BH, Lopez Rodrigo E, Picarsic J, et al. Activating mutations in CSF1R and additional receptor tyrosine kinases in histiocytic neoplasms. *Nat Med*. 2019;25(12):1839-1842.
7. Shanmugam V, Griffin GK, Jacobsen ED, Fletcher CDM, Sholl LM, Hornick JL. Identification of diverse activating mutations of the RAS-MAPK pathway in histiocytic sarcoma. *Mod Pathol*. 2019;32(6):830-843.

8. Egan C, Nicolae A, Lack J, et al. Genomic profiling of primary histiocytic sarcoma reveals two molecular subgroups. *Haematologica*. 2019;105(4):951-960.

9. Massoth LR, Hung YP, Ferry JA, et al. Histiocytic and dendritic cell sarcomas of hematopoietic origin share targetable genomic alterations distinct from follicular dendritic cell sarcoma. *Oncologist*. 2021;26(7):e1263-e1272.

10. Brown NA, Furtado LV, Betz BL, et al. High prevalence of somatic MAP2K1 mutations in BRAF V600E-negative Langerhans cell histiocytosis. *Blood*. 2014;124(10):1655-1658.

11. Chakraborty R, Hampton OA, Shen X, et al. Mutually exclusive recurrent somatic mutations in MAP2K1 and BRAF support a central role for ERK activation in LCH pathogenesis. *Blood*. 2014;124(19):3007-3015.

12. Nelson DS, Quispel W, Badalian-Very G, et al. Somatic activating ARAF mutations in Langerhans cell histiocytosis. *Blood*. 2014; 123(20):3152-3155.

13. Emile J-F, Diamond EL, Hélias-Rodzewicz Z, et al. Recurrent RAS and PIK3CA mutations in Erdheim-Chester disease. *Blood*. 2014; 124(19):3016-3019.

14. Nelson DS, van Halteren A, Quispel WT, et al. MAP2K1 and MAP3K1 mutations in Langerhans cell histiocytosis. *Genes Chromosomes Cancer*. 2015;54(6):361-368.

15. Chakraborty R, Burke TM, Hampton OA, et al. Alternative genetic mechanisms of BRAF activation in Langerhans cell histiocytosis. *Blood*. 2016;128(21):2533-2537.

16. Diamond EL, Durham BH, Haroche J, et al. Diverse and targetable kinase alterations drive histiocytic neoplasms. *Cancer Discov*. 2016;6(2):154-165.

17. Garces S, Medeiros LJ, Patel KP, et al. Mutually exclusive recurrent KRAS and MAP2K1 mutations in Rosai-Dorfman disease. *Mod Pathol*. 2017;30(10):1367-1377.

18. Haroche J, Cohen-Aubart F, Rollins BJ, et al. Histiocytoses: emerging neoplasia behind inflammation. *Lancet Oncol*. 2017;18(2): e113-e125.

19. Allen CE, Beverley PCL, Collin M, et al. The coming of age of Langerhans cell histiocytosis. *Nat Immunol*. 2020;21(1):1-7.

20. Diamond EL, Durham BH, Ulaner GA, et al. Efficacy of MEK inhibition in patients with histiocytic neoplasms. *Nature*. 2019;567(7749):521-524.

21. Haroche J, Cohen-Aubart F, Emile J-F, et al. Dramatic efficacy of vemurafenib in both multisystemic and refractory Erdheim-Chester disease and Langerhans cell histiocytosis harboring the BRAF V600E mutation. *Blood*. 2013;121(9):1495-1500.

22. Cohen Aubart F, Emile J-F, Carrat F, et al. Targeted therapies in 54 patients with Erdheim-Chester disease, including follow-up after interruption (the LOVE study). *Blood*. 2017;130(11):1377-1380.

23. Cohen Aubart F, Emile J-F, Maksud P, et al. Efficacy of the MEK inhibitor cobimetinib for wild-type BRAF Erdheim-Chester disease. *Br J Haematol*. 2018;180(1):150-153.

24. Diamond EL, Subbiah V, Lockhart AC, et al. Vemurafenib for BRAF V600-mutant Erdheim-Chester disease and langerhans cell histiocytosis: analysis of data from the Histology-Independent, Phase 2, Open-label VE-BASKET Study. *JAMA Oncol*. 2018;4(3):384-388.

25. Kieran MW, Geoerger B, Dunkel IJ, et al. A phase I and pharmacokinetic study of oral dabrafenib in children and adolescent patients with recurrent or refractory *BRAF* V600 mutation-positive solid tumors. *Clin Cancer Res*. 2019;25(24):7294-7302.

26. Donadieu J, Larabi IA, Tardieu M, et al. Vemurafenib for refractory multisystem Langerhans cell histiocytosis in children: an international observational study. *J Clin Oncol*. 2019;37(31):2857-2865.

27. Bhatia A, Hatzoglou V, Ulaner G, et al. Neurologic and oncologic features of Erdheim-Chester disease: a 30-patient series. *Neuro-oncol*. 2020;22(7):979-992.

28. Picarsic J, Pysher T, Zhou H, et al. BRAF V600E mutation in Juvenile Xanthogranuloma family neoplasms of the central nervous system (CNS-JXG): a revised diagnostic algorithm to include pediatric Erdheim-Chester disease. *Acta Neuropathol Commun*. 2019;7(1):168.

29. Chan JKC, Lamant L, Algar E, et al. ALK^+ histiocytosis: a novel type of systemic histiocytic proliferative disorder of early infancy. *Blood*. 2008;112(7):2965-2968.

30. Facchetti F, Pileri SA, Lorenzi L, et al. Histiocytic and dendritic cell neoplasms: what have we learnt by studying 67 cases. *Virchows Arch*. 2017;471(4):467-489.

31. Huang H, Gheorghe G, North PE, Suchi M. Expanding the phenotype of ALK-positive histiocytosis: a report of 2 cases. *Pediatr Dev Pathol*. 2018;21(5):449-455.

32. Tran TAN, Chang KTE, Kuick CH, Goh JY, Chang C-C. Local ALK-positive histiocytosis with unusual morphology and novel *TRIM33-ALK* gene fusion. *Int J Surg Pathol*. 2021;29(5):543-549.

33. Qiu L, Weitzman SP, Nastoupil LJ, et al. Disseminated ALK-positive histiocytosis with *KIF5B-ALK* fusion in an adult. *Leuk Lymphoma*. 2021;62(5):1234-1238.

34. Kashima J, Yoshida M, Jimbo K, et al. ALK-positive histiocytosis of the breast: a clinicopathologic study highlighting spindle cell histology. *Am J Surg Pathol*. 2021;45(3): 347-355.

35. Syrykh C, Ysebaert L, Péricart S, et al. ALK-positive histiocytosis associated with chronic lymphocytic leukaemia/small lymphocytic lymphoma: a multitarget response under ibrutinib. *Virchows Arch*. 2021;478(4):779-783.

36. Keeney MG, Flotte TJ, Macon WR. Cutaneous ALK-positive histiocytosis. *J Hematop*. 2021;14(1):89-91.

37. Zhu Y, Fan J, Pan H, et al. ALK-positive histiocytosis of the umbilicus with KIF5B-ALK fusion: a case report and review of the literature. *Hum Pathol Case Reports*. 2021;24:200504.

38. Bai Y, Sun W, Niu D, et al. Localized ALK-positive histiocytosis in a Chinese woman: report of a case in the lung with a novel EML4-ALK rearrangement [published online ahead of print 7 April 2021]. *Virchows Arch*. 2021. doi: 10.1007/s00428-021-03092-8.

39. Rossi S, Gessi M, Barresi S, et al. ALK -rearranged histiocytosis: report of two cases with involvement of the central nervous system. *Neuropathol Appl Neurobiol*. 2021; 47(6):878-881.

40. Takeyasu Y, Okuma HS, Kojima Y, et al. Impact of ALK inhibitors in patients with *ALK*-rearranged nonlung solid tumors. *JCO Precis Oncol*. 2021;5(5):756-766.

41. Osako T, Kurisaki-Arakawa A, Dobashi A, et al. Distinct clinicopathologic features and possible pathogenesis of localized ALK-positive histiocytosis of the breast [published online ahead of print 6 September 2021]. *Am J Surg Pathol*. doi: 10.1097/PAS. 0000000000001794.

42. Cuviello A, Rice J, Cohen B, Zambidis ET. Infant with a skin lesion and respiratory distress. *BMJ Case Rep*. 2018;2018:bcr-2018-224506.

43. Chang KTE, Tay AZE, Kuick CH, et al. ALK-positive histiocytosis: an expanded clinicopathologic spectrum and frequent presence of KIF5B-ALK fusion. *Mod Pathol*. 2019;32(5):598-608.

44. Wolter NE, Ngan B, Whitlock JA, Dickson BC, Propst EJ. Atypical juvenile histiocytosis with novel KIF5B-ALK gene fusion mimicking subglottic hemangioma. *Int J Pediatr Otorhinolaryngol*. 2019;126:109585.

45. Gupta GK, Xi L, Pack SD, et al. ALK-positive histiocytosis with *KIF5B-ALK* fusion in an adult female. *Haematologica*. 2019;104(11): e534-e536.

46. Lucas CG, Gilani A, Solomon DA, et al. ALK-positive histiocytosis with KIF5B-ALK fusion in the central nervous system. *Acta Neuropathol*. 2019;138(2):335-337.

47. Swain F, Williams B, Barbaro P. ALK-positive histiocytosis with peripheral blood histiocytes: a case report. *Acta Haematol*. 2021;144(2):218-221.

48. Jaber OI, Jarrah DA, Hiasat M, Hussaini MA. ALK-positive histiocytosis: a case report and literature review. *Turk Patoloji Derg*. 2021; 37(2):172-177.

49. Mehta J, Borges A. ALK positive histiocytosis in an adult female with an EML4-ALK RNA fusion. *Hum Pathol Case Rep*. 2020;21:200404.

50. Ross JS, Ali SM, Fasan O, et al. *ALK* fusions in a wide variety of tumor types respond to anti-ALK targeted therapy. *Oncologist*. 2017;22(12):1444-1450.

51. Sugiyama M, Hirabayashi S, Ishi Y, et al. Notable therapeutic response in a patient with systemic juvenile xanthogranuloma with KIF5B-ALK fusion. *Pediatr Blood Cancer*. 2021;68(11):e29227.

52. Goyal G, Shah MV, Call TG, Litzow MR, Hogan WJ, Go RS. Clinical and radiologic responses to cladribine for the treatment of

Erdheim-Chester disease. *JAMA Oncol*. 2017;3(9):1253-1256.

53. Goyal G, Abeykoon JP, Hu M, et al; Mayo Clinic-University of Alabama at Birmingham Histiocytosis Working Group. Single-agent cladribine as an effective front-line therapy for adults with Langerhans cell histiocytosis. *Am J Hematol*. 2021;96(5):E146-E150.

54. Richardson SO, Huibers MMH, de Weger RA, et al. One-fits-all pretreatment protocol facilitating fluorescence in situ hybridization on formalin-fixed paraffin-embedded, fresh frozen and cytological slides. *Mol Cytogenet*. 2019;12(1):27.

55. Benayed R, Offin M, Mullaney K, et al. High yield of RNA sequencing for targetable kinase fusions in lung adenocarcinomas with no mitogenic driver alteration detected by DNA sequencing and low tumor mutation burden. *Clin Cancer Res*. 2019;25(15):4712-4722.

56. van Dongen JJM, Langerak AW, Brüggemann M, et al. Design and standardization of PCR primers and protocols for detection of clonal immunoglobulin and T-cell receptor gene recombinations in suspect lymphoproliferations: report of the BIOMED-2 Concerted Action BMH4-CT98-3936. *Leukemia*. 2003; 17(12):2257-2317.

57. van Krieken JHJM, Langerak AW, Macintyre EA, et al. Improved reliability of lymphoma diagnostics via PCR-based clonality testing: report of the BIOMED-2 Concerted Action BHM4-CT98-3936. *Leukemia*. 2007;21(2): 201-206.

58. Ravindran A, Goyal G, Go RS, Rech KL; Mayo Clinic Histiocytosis Working Group. Rosai-Dorfman disease displays a unique monocyte-macrophage phenotype characterized by expression of OCT2. *Am J Surg Pathol*. 2021;45(1):35-44.

59. Sukov WR, Cheville JC, Carlson AW, et al. Utility of ALK-1 protein expression and ALK rearrangements in distinguishing inflammatory myofibroblastic tumor from malignant spindle cell lesions of the urinary bladder. *Mod Pathol*. 2007;20(5):592-603.

60. Rigaud C, Barkaoui MA, Thomas C, et al. Langerhans cell histiocytosis: therapeutic strategy and outcome in a 30-year nationwide cohort of 1478 patients under 18 years of age. *Br J Haematol*. 2016;174(6):887-898.

61. Héritier S, Barkaoui M-A, Miron J, et al. Incidence and risk factors for clinical neurodegenerative Langerhans cell histiocytosis: a longitudinal cohort study. *Br J Haematol*. 2018;183(4):608-617.

62. Estrada-Veras JI, O'Brien KJ, Boyd LC, et al. The clinical spectrum of Erdheim-Chester disease: an observational cohort study. *Blood Adv*. 2017;1(6):357-366.

63. Cohen-Aubart F, Emile J-F, Carrat F, et al. Phenotypes and survival in Erdheim-Chester disease: results from a 165-patient cohort. *Am J Hematol*. 2018;93(5):E114-E117.

64. Dehner LP. Juvenile xanthogranulomas in the first two decades of life: a clinicopathologic study of 174 cases with cutaneous and extracutaneous manifestations. *Am J Surg Pathol*. 2003;27(5):579-593.

65. Janssen D, Harms D. Juvenile xanthogranuloma in childhood and adolescence: a clinicopathologic study of 129 patients from the kiel pediatric tumor registry. *Am J Surg Pathol*. 2005;29(1):21-28.

66. Haupt R, Minkov M, Astigarraga I, et al; Euro Histio Network. Langerhans cell histiocytosis (LCH): guidelines for diagnosis, clinical work-up, and treatment for patients till the age of 18 years. *Pediatr Blood Cancer*. 2013;60(2): 175-184.

67. Goyal G, Heaney ML, Collin M, et al. Erdheim-Chester disease: consensus recommendations for evaluation, diagnosis, and treatment in the molecular era. *Blood*. 2020;135(22):1929-1945.

68. Xu J, Huang X, Wen Y, et al. Systemic Juvenile xanthogranuloma has a higher frequency of ALK translocations than BRAFV600E mutations [published online ahead of print 18 August 2020]. *J Am Acad Dermatol*. doi: 10.1016/j.jaad.2020.08.053.

69. Maeda M, Morimoto A, Shioda Y, et al; Histiocytosis Study Group of the Japanese Society of Pediatric Hematology/Oncology. Long-term outcomes of children with extracutaneous juvenile xanthogranulomas in Japan. *Pediatr Blood Cancer*. 2020;67(7): e28381.

70. Bhatia A, Ulaner G, Rampal R, et al. Single-agent dabrafenib for *BRAF*^{V600E}-mutated histiocytosis. *Haematologica*. 2018;103(4): e177-e180.

71. Lovly CM, Gupta A, Lipson D, et al. Inflammatory myofibroblastic tumors harbor multiple potentially actionable kinase fusions. *Cancer Discov*. 2014;4(8): 889-895.

72. Dickson BC, Swanson D, Charames GS, Fletcher CD, Hornick JL. Epithelioid fibrous histiocytoma: molecular characterization of ALK fusion partners in 23 cases. *Mod Pathol*. 2018;31(5):753-762.

73. Doyle LA, Mariño-Enriquez A, Fletcher CD, Hornick JL. ALK rearrangement and overexpression in epithelioid fibrous histiocytoma. *Mod Pathol*. 2015;28(7):904-912.

74. Cheah AL, Zou Y, Lanigan C, et al. ALK expression in angiomatoid fibrous histiocytoma: a potential diagnostic pitfall. *Am J Surg Pathol*. 2019;43(1):93-101.

75. Van Zwam P, Mentzel T, Flucke U. ALK expression in angiomatoid fibrous histiocytoma: confirmation of the findings of Cheah et al. *Am J Surg Pathol*. 2019;43(8):1156.

76. Hallberg B, Palmer RH. The role of the ALK receptor in cancer biology. *Ann Oncol*. 2016;27(suppl 3):iii4-iii15.

77. Musgrove EA, Caldon CE, Barraclough J, Stone A, Sutherland RL. Cyclin D as a therapeutic target in cancer. *Nat Rev Cancer*. 2011;11(8):558-572.

78. Ou S-HI, Greenbowe J, Khan ZU, et al. I1171 missense mutation (particularly I1171N) is a common resistance mutation in ALK-positive NSCLC patients who have progressive disease while on alectinib and is sensitive to ceritinib. *Lung Cancer*. 2015;88(2):231-234.

79. Dagogo-Jack I, Rooney M, Lin JJ, et al. Treatment with next-generation ALK inhibitors fuels plasma *ALK* mutation diversity. *Clin Cancer Res*. 2019;25(22):6662-6670.